

Fast Minimal Presentations of Bi-graded Persistence Modules *

Michael Kerber[†]Alexander Rolle[†]**Abstract**

Multi-parameter persistent homology is a recent branch of topological data analysis. In this area, data sets are investigated through the lens of homology with respect to two or more scale parameters. The high computational cost of many algorithms calls for a preprocessing step to reduce the input size. In general, a minimal presentation is the smallest possible representation of a persistence module. Lesnick and Wright [28] proposed recently an algorithm (the LW-algorithm) for computing minimal presentations based on matrix reduction.

In this work, we propose, implement and benchmark several improvements over the LW-algorithm. Most notably, we propose the use of priority queues to avoid extensive scanning of the matrix columns, which constitutes the computational bottleneck in the LW-algorithm, and we combine their algorithm with ideas from the multi-parameter chunk algorithm by Fugacci and Kerber [21]. Our extensive experiments show that our algorithm outperforms the LW-algorithm and computes the minimal presentation for data sets with millions of simplices within a few seconds. Our software is publicly available.

1 Introduction.

Motivation. Persistent homology is a multi-scale approach to extract information from a data set that would remain hidden using conventional methods. The idea is to consider the data at multiple scales and track the topological evolution as the scale changes. The success of this theory, which is a primary tool of *topological data analysis*, has been manifested in countless applications, e.g. [31, 6, 35, 30]. One major reason for this success is the existence of fast algorithms to compute the required topological invariants.

Multi-parameter persistent homology extends the above concepts by filtering the data by several independent scale parameters, rather than just one. Indeed, it is quite often natural to look at multi-dimensional parameter spaces in data analysis, and this theory allows for a more fine-grained topological analysis. As a simple ex-

ample, when studying point cloud data, it is common to “thicken” the point set (i.e., replacing points with balls of radius $r > 0$) in the single-parameter setup. Since the results of such an analysis are unstable with respect to outliers, the point cloud is usually preprocessed by removing outliers first. This preprocessing introduces another scale parameter that determines how aggressively points are classified as outliers (see, e.g., [8]).

A drawback of multi-parameter persistent homology is that one has to deal with more complicated problems, already for the case of two parameters that we consider in this work: a complete discrete topological invariant does not exist [10], making the algebraic objects richer (and more difficult) than in the single-parameter setting. This also extends to computational problems: for instance, computing the universal distance (i.e., “most meaningful” – see [27] for details) is NP-hard for two parameters, but polynomial time (and practically efficient) for one parameter [25]. For several other problems, polynomial-time algorithms have been described recently, such as for computing the matching distance [7, 24, 26], a multi-parameter kernel [14], and the decomposition of multi-parameter modules into indecomposable elements [18] as well as weaker decompositions [9]. Despite being polynomial time, the complexity bounds typically have rather large exponents and this is also reflected in poor behavior for large input sizes in practice.

To improve all aforementioned algorithms, we want to preprocess the input, reducing its size as much as possible, while retaining all the relevant homological information. Such a reduction is possible because usually, the input is given as a bi-graded simplicial complex, but for the sake of persistent homology, one is only interested in the evolution of the homology of the complex across the various bi-grades. As homology is only a coarse topological summary of a complex, we can hope for a more succinct representation.

A *minimal presentation* is such a succinct representation. In short, a presentation encodes the homology by a set of generators and relations, each of which is associated with a bi-grade. The generators create homological features at the corresponding bi-grade, and the relations turn a certain linear combination of generators trivial at their bi-grade. This data can be en-

*Supported by Austrian Science Fund (FWF) grant number P 29984-N35.

[†]Graz University of Technology, Graz, Austria

coded in a matrix where rows represent generators and columns represent relations, and each row and column also stores a bi-grade. This matrix is the main object of our studies. A presentation is called minimal if among all presentations of the same homological data, it possesses the minimal number of generators and relations (we refer to Section 2 for a precise definition).

A recent algorithm for computing minimal presentations by Lesnick and Wright [28] (the LW-algorithm, from now on) is a key component of RIVET [36], the most prominent software package supporting 2-parameter persistent homology calculations. RIVET allows for an interactive exploration of bi-filtered data sets and has received attention in various data analysis applications, including neuroscience [23, 34], physics [13], and machine learning [37].

Our contribution. We describe a fast algorithm to compute a minimal presentation. More precisely, we introduce improvements to the LW-algorithm, drastically improving its performance.

The LW-algorithm arrives at a minimal presentation by a sequence of column operations, employing a smart traversal strategy of the columns (we describe the approach in detail in Section 3). However, it turns out that the bulk of its running time is not spent on performing the actual work (i.e., the column operations), but *searching* for the work to be done.

We introduce several major improvements which are all variations of the same theme: at several occasions, the algorithm scans a range of columns in order to find which need to be updated. However, most of the scanned columns typically remain unchanged. Our observation is that those columns that need an update can be predicted by earlier steps of the algorithm, hence we can schedule them for updates (using a priority queue) and avoid the scan completely. This simple observation removes the major computational bottlenecks and leads to immense performance gains.

We obtain further speed-ups by using the multi-chunk algorithm of Fugacci and Kerber [21] as a preprocessing step: this algorithm transforms a bi-graded cell complex into a smaller bi-graded cell complex with the same persistent homology. The result is not minimal in terms of presentations, but this algorithm typically gets rid of many cells that the LW-algorithm would only remove in the last step. Hence, preprocessing results in starting the LW-algorithm with fewer rows and columns. As the chunk algorithm only needs a fraction of the runtime, the preprocessing is efficient in practice. We investigated further variants:

- We implemented a clearing optimization (that is already hinted at in [28]) to avoid certain column operations in the algorithm. Unlike in the single-

parameter case where clearing is an important tool for efficiency [4], it only yields a small improvement in our scenario. Part of the reason is that the chunk preprocessing already removes most of the potential for clearing, and it does so more efficiently.

- The algorithm consists of 5 main sub-steps, out of which 3 can be easily parallelized, and the other two are independent and can be ran parallel to each other as well. We show that parallelization yields to additional speed-ups.
- We use a matrix data structure derived from the PHAT library. As observed in [5], the column type of the matrix has a significant influence on the performance. Our implementation is generic in the column type, so that we could benchmark our approach with all columns types that PHAT offers.

We tested our C++-implementation on a variety of data sets, including triangular mesh data, bifiltered flag complexes, and others. The speed-ups obtained by our improvements are significant for all tested instances, and in many cases, the runtime and memory consumption changes from a quadratic to a near-linear empirical behavior; see Sections 4 and 5. In particular, computing the minimal presentation for complexes with millions of cells is now possible within a few seconds. Our software is called *mpfree*, and it is available.¹

Further related work. The LW-algorithm is specialized for the case of bi-graded persistence modules. However, minimal presentations can be computed for more general (graded) modules, and more general algorithms are provided by computer algebra systems like Macaulay or Singular. Lesnick and Wright [28] compare their implementation with these systems and show that their algorithm is much faster in this special case.

There are alternatives to minimal presentations to reduce the size of cell complexes. Besides the aforementioned result by Fugacci and Kerber [21], a line of research simplifies cell complexes through collapses based on Discrete Morse Theory [1, 2, 32]. These approaches empirically yield a similar compression rate as the chunk reduction, but only provide weaker theoretical guarantees in terms of minimality, and their current implementation is not as fast as the chunk algorithm.

This work is similar in spirit to several papers improving the performance of the algorithm to compute persistence diagrams in a single parameter. See [29] for a survey. Most algorithmic improvements are based on rather simple observations which nonetheless have to be combined in the right way to yield an efficient result –

¹<https://bitbucket.org/mkerber/mpfree>

the PHAT library is dedicated to studying the different algorithmic variants; see [5] for a discussion how different parameters can change the outcome drastically.

Scope. We focus in this paper on the algorithm engineering aspect of our work. That means that we introduce algebraic concepts only as much as needed to describe the algorithmic steps and our improvements, and shift the correctness proofs to the appendix.

2 Preliminaries.

Bi-Graded matrices. A *bi-grade* is an element of \mathbb{Z}^2 . A bi-grade $g = (g_x, g_y)$ is *smaller* than $h = (h_x, h_y)$, written $g \leq h$, if $g_x \leq h_x$ and $g_y \leq h_y$.

We fix the base field $K := \mathbb{Z}_2$ for simplicity, although the algorithm can be rephrased for any field K with little effort. A *bi-graded matrix* is an $(m \times n)$ -matrix over K , where each row and each column is annotated with a bi-grade such that whenever the (i, j) -entry of the matrix is 1, then $g^{(i)} \leq g^{(j)}$, where $g^{(i)}$ is the grade of the i -th row and $g^{(j)}$ is the grade of the j -th column. In what follows, we will skip the “bi”-prefix and only talk about *graded matrices* and *grades*.

We will assume that a graded matrix is stored in some sparse column representation, that is, the row indices of non-zero entries in a column are stored in some container data structure (e.g., a dynamic vector or a linked list). Also, we assume that a graded matrix always stores its rows and columns in co-lexicographic order with respect to the grades, with rows/columns of the same grade ordered arbitrarily. Note that this order is a refinement of \leq to a total order.

For a non-zero column, the *pivot* is the largest row index with non-zero entry with respect to the fixed total colex-order of rows. We call a column *local* if the grade of the pivot row equals the grade of the column.

Persistence modules. A *persistence module* is a family $(V_p)_{p \in \mathbb{Z}^2}$ of K -vector spaces for each grade, together with maps $f_{p \rightarrow q} : V_p \rightarrow V_q$ for every pair of grades with $p \leq q$ which are *functorial*, that means, $f_{p \rightarrow p}$ is the identity and $f_{q \rightarrow r} \circ f_{p \rightarrow q} = f_{p \rightarrow r}$ for $p \leq q \leq r$. The term “module” comes from the fact that this object carries the algebraic structure of a \mathbb{Z}^2 -graded module over the polynomial ring $K[x, y]$ [10, 15].

We can define persistence modules using graded matrices. Fixing a grade $p \in \mathbb{Z}^2$, let $M_{\leq p}$ denote the submatrix of M that contains the rows and columns with grades $\leq p$. Note that a graded $m \times n$ matrix M induces a linear map $K^n \rightarrow K^m$ by matrix-vector multiplication, and the same is true for $M_{\leq p}$, adjusting the dimensions of domain and co-domain to the dimension of the submatrix. We call a pair (A, B) with A an $\ell \times n$ and B an $n \times m$ -matrix a *free implicit representation (firep)* if the row grades of A coincide with the column

grades of B , and $BA = 0$. In that case, for every p , also $B_{\leq p}A_{\leq p} = 0$ holds, implying that the image of $A_{\leq p}$ is contained in the kernel of $B_{\leq p}$. Hence we can define

$$V_p := (\ker B_{\leq p}) / (\text{im } A_{\leq p})$$

and $f_{p \rightarrow q}$ to be map that assigns to an element of $\ker B_{\leq p}$ an element of $\ker B_{\leq q}$ by padding additional dimensions with zeros. Note that this construction, despite its algebraic formalism, is very natural in practice: Given a bi-graded simplicial complex C and a dimension d , picking for A the $((d+1), d)$ -boundary matrix and for B the $(d, (d-1))$ -boundary matrix yields a free implicit representation. For readers unfamiliar with these concepts, we refer to Appendix A for more explanations.

A single graded $(m \times n)$ -matrix M can be interpreted as a persistence module: the persistence module defined by the firep $(M, 0)$. In detail: denoting $B := \{b_1, \dots, b_m\}$ as basis elements of K^m , we grade b_i with the i -th row grade of M . We interpret every column of M as a relation, a linear combination r_i of elements in B , yielding $R = \{r_1, \dots, r_n\}$. Then, we set

$$V_p := \langle B_{\leq p} \rangle / \langle R_{\leq p} \rangle$$

where $\langle B_{\leq p} \rangle$ is the span of all basis vectors that have grade $\leq p$ and, likewise, $\langle R_{\leq p} \rangle$ is the span of all relations at grade $\leq p$. The linear maps $V_{p \rightarrow q}$ are induced by the natural inclusions $B_{\leq p} \rightarrow B_{\leq q}$. This interpretation of a graded matrix as persistence module is called a *presentation* of a graded module, where the set B is called the *generators* and set R is called the *relations* of the presentation. A presentation is *minimal* if among all possible presentations of the persistence module (V_p) , it has the smallest number of generators and relations. We provide more algebraic background on this at the beginning of Appendix B.

Experimental setup. We will interleave the algorithmic description and the experimental evaluation to show the impact of our improvements. Our implementation is written in C++, compiled with gcc-7.5.0, and ran on a workstation with an Intel(R) Xeon(R) CPU E5-1650 v3 CPU (6 cores, 3.5GHz) and 64 GB RAM, running GNU/Linux (Ubuntu 16.04.5). We measured the overall time and memory consumption using the linux command `/usr/bin/time`, and the `timer` library of the BOOST library to measure the time for subroutines. The published version of our software has benefited from low-level improvements since we ran these experiments, but the performance is not significantly different. The input data and the benchmark scripts are available on request.

In Sections 3 and 4, we will use running examples generated by the convex hull of n points on a sphere

sampled uniformly at random. By Euler’s formula, the convex hull consists of exactly $e = 3n - 6$ edges and $f = 2n - 4$ triangles. This yields a free implicit representation (A, B) , where A is the $(e \times f)$ -boundary matrix for triangles and edges, and B the $(n \times e)$ -boundary matrix for edges and vertices. The grades of a vertex are simply its x - and y -coordinates (ignoring the z -coordinate), and the x -/ y -grades of an edge and a triangle is just the maximal x -/ y -coordinate among its boundary vertices (the fact that the grades are in \mathbb{R}^2 rather than \mathbb{Z}^2 does not make a difference because there are only finitely many of them and so they can be mapped bijectively to \mathbb{Z}^2 preserving orders). This is also known as the *lower star (bi-)filtration* which generalizes a commonly used filtration type for a single parameter and has been used as a benchmark example in previous multi-parameter work [32, 21]. We also performed experiments on various other types of data and our speed-ups significantly improve all tested instances; we report on this in Section 5. For all randomly generated data sets, the listed results are averaged over 5 random instances of the same size.

3 The Lesnick-Wright Algorithm.

We rephrase the algorithm from [28] in combinatorial terms. While doing that, we try to give some intuition about why certain steps are performed in the algorithm; we refer to the original paper for correctness proofs.

Overview. The input of the LW-algorithm is a free implicit representation (A, B) , and the output is a minimal presentation matrix M .

The algorithm consists of 4 steps, where the first 3 steps convert the firep (A, B) into a presentation matrix M' (called *semi-minimal* in [28]), and the last step minimizes M' into M . We describe the four steps on a high level first:

Min_gens: Computes a minimal ordered set of generators G of the image of A . More precisely, the generators are graded, so that this encodes the image of $A_{\leq p}$ for every p .

Ker_basis: Computes a basis K of the kernel of B . More precisely, the basis elements are graded, so that the basis encodes the kernel of $B_{\leq p}$ for every p .

Reparam: Re-expresses every element of G as a linear combination in K , keeping its grade. This is possible since $BA = 0$. The resulting graded matrix M' is a semi-minimal presentation of the persistence module.

Minimize: Identifies pairs (g, r) of generators (rows in M') and relations (columns in M') where r “eliminates” g and both r and g have the same grade. In that case, row g and column r are removed

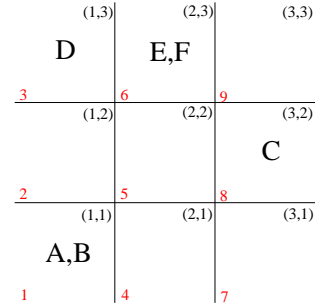


Figure 1: The grid representation of the matrix Ex_1 from above. The red numbers (lower left corner per cell) show the order in which the cells are visited by the algorithms `Min_gens` and `Ker_basis`.

from M' after some algebraic manipulations without changing the persistence module. Removing all such pairs results in a minimal presentation M .

We need to describe the algorithmic details of every step in order to explain our contributions. We also provide pseudocode in Appendix E to complement our textual description, and will frequently refer to it. We assume that every x -coordinate of a grade in A and of B is in $\{1, \dots, X\}$ and every y -coordinate in $\{1, \dots, Y\}$. Hence, we can visualize A and B via a $X \times Y$ integer grid, where each grid cell contains a (possibly empty) sequence of matrix columns. Traversing the grid row by row upwards yields the co-lexicographic order of the matrix. We will phrase the algorithms for `Min_gens` and `Ker_basis` with this interpretation.

As an example, consider the graded matrix

	A	B	C	D	E	F
	(1, 1)	(1, 1)	(3, 2)	(1, 3)	(2, 3)	(2, 3)
$Ex_1 :=$	0	1	0	1	0	0
	0	1	0	0	0	0
	1	0	0	0	1	1
	0	0	1	0	0	1
	0	0	1	0	1	0

(we skip the row grades for simplicity). Its representation as a grid is depicted in Figure 1.

Details of Min_gens. The procedure traverses the columns of A in a certain order defined below. During the traversal, it maintains a *pivot map* ρ , a partial map from row indices to column indices. The interpretation is that $\rho(i) = j$ if column j has been visited, has pivot i , and there is no visited column j' with pivot i and $j' < j$. Initially, ρ is the empty map, reflecting the state that no column has been visited.

At any point of the algorithm, *reducing* a column j means the following operation (Alg. 1): as long as j is

not empty, has pivot i and $\rho(i) = j'$ with $j' < j$, add column j' to column j . This results in cancellation of the pivot (since the coefficients are over \mathbb{Z}_2) and hence, after the addition, the pivot of j is strictly smaller than i (or the column is empty). In either case, the reduction terminates after finitely many iterations, and column j is marked as visited. If it ends with a non-empty column with pivot i , set $\rho(i) \leftarrow j$.

We can now describe the procedure `Min_gens` (see Alg. 2): Using the grid interpretation from above, traverse the grid cells in lexicographic order; that means, the grid is traversed column by column from the left, traversing each column bottom-up. When reaching grid cell (x, y) , iterate through all matrix columns with grade $(1, y), (2, y), \dots, (x - 1, y)$ in that order (i.e., through all cells on the left of (x, y)) and reduce them as described above. Then, iterate through the matrix columns at grade (x, y) and reduce them as well. Append every column at grade (x, y) not reducing to 0 in the output matrix, with grade (x, y) .

Details of `Ker_basis`. This procedure is similar to the previous one, as it visits the columns in the same order, and reduces them when visiting. There is one difference in the reduction procedure, however: every column maintains an *auxiliary vector*. Initially, the auxiliary vector of column j is just the unit vector e_j and whenever column j' is added to column j , we also add the auxiliary vector of j' to the auxiliary vector of j . In linear algebra terms, the auxiliary vectors yields an auxiliary matrix S (which is the identity matrix initially) and letting B' denote the matrix arising from B at any point of the algorithm, we maintain the invariant that $B' = BS$ (in [28], the auxiliary matrix is called the “slave matrix”). In particular, if the j -th column of B' is 0, the j -th column of S encodes the linear combination of the columns of B that represents a kernel element of the linear map B .

We describe the procedure `Ker_basis` (Alg. 3): Traverse the grid cells in lexicographic order. When reaching grid cell (x, y) , iterate through all matrix columns with grade $(1, y), (2, y), \dots, (x, y)$ (in that order) and reduce them as described above. If any of these columns turn from non-zero to zero during the reduction, append the auxiliary vector of the column to the output matrix and set the grade of this column to (x, y) . The resulting matrix encodes the kernel basis of B . Its rows correspond to the columns of B and thus inherit their grades, yielding a graded matrix as output.

As an example, we apply the algorithm to the matrix Ex_1 in Figure 1. When visiting grade $(2, 3)$, column C is not visited yet, so the algorithm update $\rho(5) \leftarrow E$ and $\rho(4) \leftarrow F$. When reaching grade $(3, 2)$, visiting column C , it does not perform a column

operation because E is after C in colexicographic order. So, $\rho(5) \leftarrow C$ is set and the algorithm continues. At grade $(3, 3)$, the algorithm re-reduces columns D , E , and F again. In particular, when reducing E , it updates $E \leftarrow C + E$, updating its pivot to 4, and setting $\rho(4) \leftarrow E$. Then when updating F , it updates $F \leftarrow E + F$, which is equal to 0. The corresponding auxiliary vector is $(0, 0, 1, 0, 1, 1)^T$. Hence, the result is a kernel element representing $C + E + F$, at grade $(3, 3)$.

Details of `Reparam`. Let G denote the result of `Min_gens` and K the result of `Ker_basis`. Note that G and K have the same number of rows, with consistent grades. Form the matrix $(K|G)$ and reduce each column of G , using auxiliary vectors. It is guaranteed that this turns the matrix into $(K|0)$, and the auxiliary vectors of the columns of G yields a graded matrix M' which is the output of the procedure (Alg. 4).

Details of `Minimize`. Let n denote the number of columns of M' , the output of the previous step. Traverse the columns of M' from index 1 to n . If column i is a local column (i.e., the grade of its pivot coincides with the column grade), let j denote its pivot and iterate through the columns $i + 1$ to n ; if any column k contains row index j , add column i to column k (eliminating the row index at j). At the end of this inner loop, no column except i has a non-zero entry at index j . We can therefore remove column i and row j from the matrix, without changing the persistence module that M' presents. So, remove column i and row j from the matrix. After the outer loop has finished, re-index the remaining rows and columns, and return the resulting graded matrix M as the minimal presentation (Alg. 6).

As an example, consider the graded matrix

		A	B	C	D	E
		$(1, 1)$	$(2, 1)$	$(3, 1)$	$(3, 3)$	$(3, 3)$
$Ex_2 :=$	S	$(1, 1)$	0	1	0	0
	T	$(1, 1)$	1	0	1	0
	U	$(1, 1)$	1	1	1	0
	V	$(3, 1)$	0	0	1	1
	W	$(3, 3)$	0	0	0	1

The algorithm identifies A as a local column and adds it to columns B , C , and D . B is a non-local column on which the algorithm does nothing. C is local also after adding A , and the (modified) C is added to D . Since D is still local, it gets added to E , turning E into a

n	RIVET		Our RIVET “clone”	
	Time	Memory	Time	Memory
7.5K	15.6	3.10GB	3.76	468MB
15K	62.5	12.3GB	17.6	1.82GB
30K	353	49.3GB	71.6	7.17GB
60K	–	>64GB	385	28.4GB

Table 1: Time (in seconds) and memory consumption of the algorithm in RIVET, and our version of it (“Clone”) for the convex hull dataset. The letter K stands for thousands. For 60K points, RIVET ran out of memory, and our version used up around 45% of the memory.

non-local column. In the end, we obtain

		A	B	C	D	E	
		(1, 1)	(2, 1)	(3, 1)	(3, 3)	(3, 3)	
$Ex'_2 :=$	S	(1, 1)	0	1	0	0	1
	T	(1, 1)	1	1	0	1	0
	U	(1, 1)	1	0	0	0	0
	V	(3, 1)	0	0	1	0	0
	W	(3, 3)	0	0	0	1	0

and the minimal presentation is obtained by removing rows U , V , and W and columns A , C , and D .

Performance. The algorithm described in this section is implemented in the RIVET library². We have implemented our own version of the algorithm, for the sake of easier integration of the improvements that follow. Our algorithm produces precisely the same output file as RIVET in all tested instances. Table 1 shows the runtime and memory comparison of the two implementations. We also compared for other types of input, and the two versions consistently vary by a factor of 2-10 in speed, and 1-8 in memory, probably due to low-level implementation differences. Therefore, we consider our implementation as a valid proxy for RIVET, and omit further comparisons with RIVET for the rest of the paper.³

4 Improvements.

We describe methods to significantly improve several steps of the LW-algorithm. We introduce them one by one and show the effect on the algorithmic performance using the running example from last section.

Queues. From Table 1, we can easily infer a quadratic complexity of the algorithm in the size of the initial presentation, both in time and memory. The reason for that, however, is not the cost of the performed column operations but the sheer size of the grid

used in `Min_gens` and `Ker_basis`. Since the points on the convex hull are chosen randomly, the size of the grid is roughly $n \times n$, and both our algorithm and the RIVET version store the grid as a two-dimensional array containing some data for each grid cell, leading to this quadratic behavior. We point out that even if we avoid constructing this array, just iterating over every grid cell will still lead to quadratic runtime. The obvious “solution” of defining a coarser grid and snapping each grade to the closest coarse grid cell is not satisfying because it only offers an approximate solution; on top of that, it is not clear how to choose the coarser grid. We show that coarsening is not necessary, as the algorithm can be adapted to be indifferent about the grid size in terms of performance:

First note that although the grid is of size $n \times n$ in our example, only $O(n)$ of the grid cells appear as grades of columns of the matrix. On the other hand, it is not sufficient to only consider these grades in `Min_gens` and `Ker_basis`. For instance, columns of B on grades (x', y) and (x, y') with $x' < x$ and $y' < y$ might combine into a kernel element at grade (x, y) , so `Ker_basis` has to perform work at grade (x, y) even if no column exists at this grade. An example for this is the matrix Ex_1 from Figure 1, where a kernel element appears on grade $(3, 3)$ as a combination of C , E , and F .

The main observation is that we can predict the grades on which the algorithm has to (potentially) perform operations, effectively avoiding to iterate through all grid cells. Surely, every grade that appears as a grade of matrix columns must be considered, to visit these columns for the first time. Moreover, consider the situation that the algorithm is at grade (x, y) and reduces a column with index i . Assume further that the pivot j of i appears already in ρ for an index $k > i$. In that case, the LW-algorithm updates $\rho(j) \leftarrow i$ and stops the reduction. However, we know more: the next time that column k is visited, column i , or perhaps some other column with pivot j , will be added to k . When is this next time? Since $i < k$ and the columns are in colex order, we know that y , the y -grade of i , is smaller or equal y' , the y -grade of k . If $y' = y$, column k will be handled in the same iteration, and nothing needs to be done. If $y' > y$, we know that the algorithm needs to consider grade (x, y') . In the example Ex_1 , this case appears when considering column C at grade $(3, 2)$, having the same pivot as E at grade $(2, 3)$, which means that grade $(3, 3)$ needs to be considered.

Based on this idea, we set up a priority queue that stores the grid cells that need to be visited, in lexicographic order. The queue is initialized with the column grades of the matrix. Then, instead of iterating over all grid cells, the algorithms `Min_gens` and `Ker_basis` keep

²<https://github.com/rivetTDA/rivet>

³We remark that we run RIVET sequentially in our tests, but parallelizing does not change the outcome significantly.

popping the smallest element from the queue until the queue is empty, and proceed on each grade as described before. We extend the reduction method of a column as follows (Alg. 8): Whenever the algorithm encounters a situation as above during a column reduction, it pushes (x, y') to the queue. Every element pushed to the queue is necessarily lexicographically larger than the current element, so the algorithm terminates – in the worst case after having handled every grid cell once, but skipping over many grid cells in practice. In the example Ex_1 , the queue would be initialized with the four grades $(1, 1), (3, 2), (1, 3), (2, 3)$, and only the grade $(3, 3)$ would be pushed into the queue during the run.

A further improvement is based on a very similar idea: note that when a grade (x, y) is handled, both `Min_gens` and `Ker_basis` still scan through all columns of grade (x', y) with $x' \leq y$ and reduce all columns in this range. Since only a few columns in this range typically need an update, most of the time in the algorithm is wasted for scanning through this range.

Necessary updates can be predicted during earlier steps in the algorithm: as above, when, at grade (x, y) column i is reduced and its pivot is found in a column $k > i$, we know that column k needs an update. Let $y' \geq y$ be the y -grade of k . We can just remember the index k and handle it the next time when y -grade y' is visited (which will be for grade (x, y')).

Technically, we realize this idea by storing one priority queue per y -grade. In the extended column reduction, in a situation as above, the index k is pushed to the priority queue of its y -grade. When handling a grade (x, y) , instead of scanning through the columns of grade $(1, y), \dots, (x - 1, y)$, we keep popping the smallest index from the priority queue of y and reduce the column (this might introduce new elements to the priority queue, if $y = y'$ with the notation from above, but new elements are of larger index, so the procedure eventually empties the queue). After the queue is empty, the algorithm proceeds with the columns on grade (x, y) as in the LW-version. See Alg. 9 and 10 for pseudocode.

It is not difficult to see that these variants perform exactly the same column operations as the original versions of `Min_gens` and `Ker_basis` (see Appendix B). For instance, in the example matrix Ex_1 , visiting column C triggers to push column E in the priority queue for y -grade 3. At grade $(3, 3)$, E is popped from the queue (skipping column C), and reducing E leads to pushing column F into the queue, which in turn is reduced to 0 as in the original algorithm.

In Table 2, we see a substantial improvement both in time and memory when using priority queues. In particular, the memory consumption is close to linear.

n	Our RIVET “clone”		Using queues	
	Time	Memory	Time	Memory
7.5K	3.76	468MB	0.70	32MB
15K	17.6	1.82GB	2.72	72MB
30K	71.6	7.17GB	10.8	153MB
60K	385	28.4GB	54.6	370MB

Table 2: Running time and memory comparison for the original algorithm and the variant using queues to avoid extensive scanning.

Lazy minimization. Despite the improvement using queues, Table 2 shows that the practical runtime complexity is still quadratic. The reason for that lies in the minimization procedure: In Table 3, we show the running time of the sub-step separately, and it is evident that it is the computational bottleneck of the algorithm (when using the queue-improvement).

Recall that in the LW-minimization, whenever it identifies a local pair, the algorithm scans to the right to eliminate the local row index. This scan is responsible for the observed quadratic time complexity. Typically, the row index only appears in a few columns, and the scan will query many columns that are not updated. Additionally, looking for a fixed row index is a non-constant operation for most representations of column data. For instance, if the column is realized as a dynamic array, it requires a binary search per column.

Our improvement avoids both scanning and binary search by not eliminating local row indices immediately when they are identified as local (this explains the name “lazy”). Instead, we first determine all local row and column indices and then we remove them “in bulk” in a second step. As we prove in Appendix B, despite performing a different set of column additions in general, the resulting presentation matrix is still minimal (this optimization has been already hinted at in [28, Remark 4.4]). The detailed algorithmic description follows (Alg. 11):

Let M' denote the semi-minimal presentation from the `Reparam` step. Traverse its columns in increasing index order. At column i , reduce the column (by adding columns from the left that remove its pivot), but stop the reduction as soon as the column is not local anymore. If column i is still local after that reduction, let j denote its pivot and label column i and row j as local. Then proceed with the next column.

Afterwards, iterate through all columns not labeled as local. Traverse the non-zero indices of a column i , in decreasing order. If a row index j is not labeled as local, keep it and proceed with the next (smaller) index. If j is local, set $k \leftarrow \rho(j)$. Add column k to column i , removing the local index j . This operation

n	LW-minimization		Lazy minimization	
	Total	Minimize	Total	Minimize
7.5K	0.70	0.56	0.15	0.00
15K	2.72	2.40	0.33	0.01
30K	10.8	10.1	0.73	0.02
60K	54.6	53.1	1.62	0.07

Table 3: Running times (in seconds) of the algorithm with the original and the lazy minimization procedure (both versions use the queue-optimization).

will not change the row indices $> j$ because j is the pivot of column k . Proceed with the next row index smaller than j . At the end of this procedure, column i does not contain local row indices anymore. At the end of the entire procedure, all non-local columns only contain non-local row indices. Remove all local columns and local rows from M' , re-index rows and columns, and return the resulting matrix as minimal presentation.

We apply our algorithm on the example matrix Ex_2 from before. In the first step of the algorithm, columns A , C , and D get labeled as local, as well as rows U , V , and W . Moreover, column D is added to E , resulting in $E \leftarrow (1, 1, 1, 1, 0)^T$. The reduction stops because E is not local anymore after this addition.

In the second iteration, the algorithm re-visits the non-local columns B and D . For B , which has pivot U , it adds columns A , because $((U, A)$ is a local pair). This results in $(1, 1, 0, 0, 0)^T$, and no more column addition is performed on B because S and T are both non-local rows. For column E (which has pivot V at this point), column C is added, resulting in $E = (1, 0, 0, 0, 0)$, and the algorithm stops because S is local. Note that the resulting columns B and E are the same as in the matrix Ex'_2 with the LW-procedure.

Table 3 shows the effect of the new minimization procedure, essentially turning the minimization step from the computational bottleneck to an operation whose running time is negligible. The memory consumption of the algorithm does not change significantly, so we omit the numbers. Interestingly, we observed that the total number of column additions performed by the lazy minimization is typically slightly larger than in the original method (unlike in our example matrix Ex_2 above). This underlines that the observed speed-up is due to avoiding scanning the matrix repeatedly and not due to saving matrix operations.

Chunk preprocessing. We use the multi-chunk algorithm from [21] as initial step of our minimal presentation algorithm. Strictly speaking, this is not an improvement of the LW-algorithm, as it only replaces the input matrices (A, B) with (smaller) matrices (A', B') that yield an isomorphic persistence module. The basic

idea is to identify row-column-pairs in A whose removal does not affect the persistence module, just as in the minimization step. However, we try to do so early in the process, hopefully removing a significant number of pairs upfront, so that the subsequent steps of the algorithm can operate on smaller matrices.

The details of the chunk algorithm have already been described in the lazy minimization step from above: just replace the matrix M' with A . Additionally, when removing row j from A at the end of algorithm, remove column j from B as well. After re-indexing, we obtain matrices (A', B') which are the output of the chunk reduction.

We see in Table 4 (first two lines per instance) that the chunk reduction is fast and improves the performance of all subsequent steps, resulting in a speed-up of roughly a factor of 2 in this example. Perhaps more importantly, also the memory usage drops by a factor 4 (with both factors getting gradually better for larger instances). The total number of columns of A' and B' is consistently around a quarter of those of (A, B) which is in accordance to the memory savings.

Parallelization. The main loops in the procedures `chunk_preprocessing`, `reparam`, and `minimize` can be easily parallelized in shared memory: removing the local row indices of a non-local column only requires reading access to local columns and can be performed independently for every non-local column. Similarly, re-expressing a generator in terms of a kernel basis in `reparam` can be done for all generators in parallel.

In Table 4, the third line per instance shows the effect of parallelization in the examples (we used OPENMP for the parallelization). We can see only a marginal effect for large instances. However, we will show in Section 5 that parallelization brings a more substantial speed-up in other types of instances.

The procedures `Min_gens` and `Ker_basis` do not permit an easy parallelization scheme, but since they act independently on the matrices A and B , they can be run in parallel on two cores (of course, yielding a speed-up factor of at most 2). We do not provide tabular data for this version, but it can be easily derived from the “+parfor” lines in Table 4, just subtracting the time in the “MG” column (the memory consumption is unaffected by this parallelization).

Clearing. We implemented one more optimization for `Ker_basis` reminiscent of the clearing optimization in the single parameter case [11, 4]. However, this clearing optimization takes no effect in our running example. In Appendix D, we describe the optimization and present one example with a (modest) speed-up.

n	Variant	IO	Ch	MG	KB	RP	Min	Time	Mem	Size
200K	queue,lazy	2.67	-	0.71	2.06	0.67	0.34	6.61	1.53GB	(477.6, 476.6)
	+chunk	2.50	0.23	0.06	0.45	0.06	0.01	3.38	421MB	
	+parfor	2.53	0.22	0.06	0.46	0.03	0.01	3.38	420MB	
400K	queue,lazy	5.55	-	1.70	4.74	1.53	0.81	14.5	3.49GB	(698.4, 697.4)
	+chunk	5.18	0.49	0.18	1.07	0.13	0.03	7.19	835MB	
	+parfor	5.19	0.44	0.18	1.08	0.07	0.02	7.10	834MB	
800K	queue,lazy	11.2	-	4.01	10.8	3.51	1.94	32.0	7.78GB	(1022.0, 1021.0)
	+chunk	10.4	0.99	0.50	2.47	0.28	0.08	14.9	1.62GB	
	+parfor	10.4	0.88	0.49	2.49	0.13	0.05	14.7	1.61GB	
1.6M	queue,lazy	21.9	-	9.36	24.9	8.54	4.84	70.8	17.7GB	(1520.6, 1519.6)
	+chunk	20.3	2.00	1.40	5.60	0.64	0.20	30.6	3.07GB	
	+parfor	20.1	1.74	1.36	5.64	0.30	0.17	29.7	3.12GB	

Table 4: Time and memory consumption of the algorithm (on the convex hull dataset) regarding chunk optimization and parallelization of for-loops. Columns from left to right: Input size, algorithm that was used, running times in seconds for setting up the graded matrices from input, and writing the result to output (IO), chunk preprocessing (Ch), min-gens (MG), ker-basis (KB), reparameterization (RP), minimization (Min), total time (Time), memory consumption (Mem), and the size of the output (Size). In the “Variant” column, the additions are cumulative, e.g. “+chunk” means that the option is used also in the subsequent line.

5 Further experimental evaluation.

In this section, we summarize experimental comparisons between the LW-algorithm and our improved version. We consider many types of input, since the asymptotic behavior of both the LW-algorithm and our improved version can vary significantly across different input types. For the function-Rips data (explained below), our improvements led to a constant factor runtime improvement of around 10 in the largest example; for all other types of input, our improvements led to an asymptotic runtime improvement.

Function-Rips data. We created bi-graded data sets of various sizes in the following way: we sampled n points from a noisy circle and consider the simplicial complex consisting of all n points, $e = \binom{n}{2}$ edges and $f = \binom{n}{3}$ triangles. Unlike in the previous example, the resulting matrices (A, B) are very imbalanced, and the size of the input is dominated by f , the number of columns of A . The first coordinate of the bi-grade is 0 for vertices, the distance between endpoints for edges, and the length of the longest edge for triangles. This is the *Vietoris-Rips complex*, one of the most prominent complexes in topological data analysis. For the second grade coordinate, we used a kernel density estimate with Gaussian kernel with fixed bandwidth for the vertices, and this is extended to edges and triangles by assigning the maximal value among the boundary vertices. The construction ensures that the subcomplex at each grade is a *flag complex*, that is, a complex that is completely determined by its vertices and edges.

Also by construction, the number of x -grades in

these instances is around e , and the number of y -grades is around n . This implies that the grid size is comparable to the number of columns.

The experimental results are displayed in Table 5. We observe that the bulk of running time is spent in the `Min_gens` procedure. We also notice that our queue optimization still has a significant effect, but not as strong as in the example from the last section. To explain this, note that from the $\binom{p}{3}$ columns in A , only $\binom{p}{2}$ can give rise to a relation; the remaining ones will be reduced to 0 in `Min_gens`, and a large part of the algorithm is spent to perform these reductions; this part will not be short-cut by our improvements. In other words, in comparison to the previous example, more time is spent on actual matrix operations.

We also see that using chunk-preprocessing has hardly any effect on time, but roughly doubles the memory consumption. This is not too surprising because the number of row/column-pairs that are removed is insignificant with respect to the total number of columns in A . That means that the pair (A', B') is of the same size as (A, B) , and our implementation deletes (A, B) after having generated (A', B') , leading to a doubling of memory (a more careful implementation could avoid representing both matrix pairs at the same time and save this memory overhead). However, some speed-ups are obtained by parallelization because some of the unavoidable reduction steps can be performed in parallel using chunk preprocessing, although this leads to a further increase in memory consumption. In summary, we see a running time improvement of a factor of around

N	Variant	IO	Ch	MG	KB	RP	Min	Time	Mem	Size
1.02M	rivet_clone	1.14	-	17.4	0.41	0.02	1.57	20.6	482MB	(72.2, 48.2)
	+queue,lazy	1.14	-	5.24	0.02	0.02	0.00	6.46	488MB	
	+chunk	1.16	3.94	1.51	0.00	0.00	0.00	6.64	828MB	
	+parfor	1.16	1.81	1.66	0.00	0.00	0.00	4.67	1.00GB	
2.05M	rivet_clone	2.34	-	59.0	1.01	0.04	5.06	67.6	1.01GB	(105.6, 67.8)
	+queue,lazy	2.32	-	13.1	0.05	0.04	0.00	15.6	1.01GB	
	+chunk	2.33	9.94	3.83	0.00	0.00	0.00	16.1	1.84GB	
	+parfor	2.32	4.34	4.16	0.00	0.00	0.00	10.9	2.27GB	
4.11M	rivet_clone	4.67	-	182	2.44	0.07	14.1	204	2.19GB	(123.0, 85.4)
	+queue,lazy	4.65	-	33.4	0.09	0.06	0.01	38.3	2.20GB	
	+chunk	4.69	25.1	9.12	0.00	0.00	0.00	39.0	4.05GB	
	+parfor	4.62	10.3	9.64	0.00	0.00	0.00	24.7	5.02GB	
8.17M	rivet_clone	9.36	-	554	5.90	0.13	40.5	610	4.93GB	(175.6, 121.0)
	+queue,lazy	9.33	-	93.5	0.17	0.12	0.02	103	4.94GB	
	+chunk	9.42	66.0	26.5	0.01	0.00	0.00	102	9.43GB	
	+parfor	9.44	25.6	27.7	0.01	0.00	0.00	63.2	12.1GB	

Table 5: Time and memory consumption for the function-Rips dataset. $N := \ell + n$ is the total number of columns in A and B . The meaning of the other columns is the same as in Table 4.

10 in the biggest example.

Additional mesh data. We also tested with triangular mesh data used in [21], publicly available at the AIM@SHAPE repository⁴. The graded input matrices (A, B) were generated in the same way as for the sphere meshes in Section 4.

The outcome confirms the results from Section 4: the original version runs out of memory for all but the smallest instances, and our improved version can handle all meshes within a few seconds, using only a fraction of the memory. For details, see Table 8 in Appendix C.

Random Delaunay triangulations. We tested a variant of the mesh example: we sampled n points inside the unit sphere, and we computed the Delaunay triangulation of these n points (using CGAL [22]). As before, we assign to vertices their x - and y -coordinates as grades, and to edges, triangles, and tetrahedra using the maximal grade of the boundary vertices. We have two choices to generate a free implicit representation (A, B), either using the vertices, edges, and triangles, or using edges, triangles, and tetrahedra. These two options correspond to computing a representation of (homology) dimension 1 and 2, and we refer to them as the $d = 1$ and $d = 2$ case, respectively.

We tested both cases and list the numbers in Tables 9, 11, 10, and 12 in Appendix C. In both cases, using queues and lazy minimization has a tremendous effect on the performance. Remarkably, chunk preprocessing has a very different effect: for $d = 2$, it saves runtime (and yields an asymptotic improvement), whereas

for $d = 1$, it actually increases the runtime. However, when parallelizing, the overall performance is better with the chunk optimization.

Multi-cover filtrations We also tried our algorithm on bifiltrations coming from multi-covers of point clouds: the simplicial complex at grade (r, k) represents the region of the plane covered by at least k balls of radius r around the input points; see [19] for more details. Different from the previous examples, the grid for these examples is very narrow, with only 10 different grades in y -directions. Despite the small-sized grid, using queues has a significant effect in practice, as well as lazy minimization and chunk preprocessing. Interestingly, this is the only type of example where we could see a (small) improvement when using the clearing optimization, discussed in Appendix D. We give numbers in Tables 13 and 14 in Appendix C.

Matrix data structure. Our implementation uses the `boundary_matrix` data structure of the PHAT library to store graded matrices. One of the advantages of that is that PHAT’s matrix type is generic in the column representation. In all our experiments above, we have used dynamic arrays (`vector_vector` in PHAT). Our code allows one to simply exchange the column type with any of the 7 other types that PHAT provides – see [5] for a description of them.

We repeated some of the previous experiments, trying all the different column types from PHAT, producing data similar to [5, Table 1–7]. The result is that the `vector_vector` column type is the fastest in most cases, although `bit_tree_pivot_column` (which is the default representation in PHAT) is competitive and sometimes

⁴available at <http://visionair.ge.imati.cnr.it/>

faster, at least when the algorithm runs in parallel. The experimental data is in Table 15 in Appendix C.

6 Conclusion.

We described several improvements to the Lesnick-Wright algorithm that make the computation of minimal presentations of bi-graded persistence modules very fast in practice. Some of our improvements are reminiscent of similar techniques in single-parameter persistence, namely the chunk preprocessing and the clearing method. If one is interested in minimal presentations in all homology dimensions, another form of clearing seems possible, where the information in dimension $(d + 1)$ is used to clear out columns from A without reducing them (as in [11] for one parameter). For Vietoris-Rips filtrations, this works well together with dualizing the filtration, that is, computing persistent cohomology instead [16], culminating in specialized very fast implementations for Vietoris-Rips complexes [3]. It is not clear how this “duality trick” can be carried over to the multi-parameter setup.

We plan to integrate our algorithm into a larger pipeline for 2-parameter persistence. In this, the minimal presentation is preceded by a method to generate a bi-graded simplicial complex (possibly with approximate methods), and succeeded by an algorithm to analyze the data set that the presentation represents. We want to show that passing to a minimal presentation is a crucial step to make such a pipeline feasible for realistic problem sizes. The last columns of Tables 4 and 5 show that minimal presentations are typically small compared to the input size, giving us hope that subsequent algorithms will profit a lot from this simplification.

A further natural extension is to design a minimal presentation algorithm for 3 and more parameters. An obstacle to this extension is that, in algebraic terms, the kernel of a map between free modules need not be free for 3 or more parameters. This fact is crucial for the correctness of the `ker_basis` method. Dey and Xin [18] describe an algorithm to compute a presentation in the general case, but not necessarily a minimal one, and an efficient implementation is missing.

Our approach is an instance of “lossless compression”: the persistence module encoded in the output is isomorphic to the one of the input. In the single-parameter case, a popular research direction is the approximation of persistence diagrams, where the input is reduced in a way that the resulting module is provably close to the original one in terms of bottleneck distance (e.g., [33, 17, 12]). The prospects of this idea are unexplored in the multi-parameter setup.

References

- [1] Madjid Allili, Tomasz Kaczynski, and Claudia Landi. Reducing complexes in multidimensional persistent homology theory. *Journal of Symbolic Computation*, 78:61–75, 2017.
- [2] Madjid Allili, Tomasz Kaczynski, Claudia Landi, and Filippo Mazoni. Acyclic partial matchings for multi-dimensional persistence: Algorithm and combinatorial interpretation. *Journal of Mathematical Imaging and Vision*, pages 1–19, 2018.
- [3] Ulrich Bauer. Ripser: efficient computation of Vietoris-Rips persistence barcodes. arXiv:1908.02518, 2019.
- [4] Ulrich Bauer, Michael Kerber, and Jan Reininghaus. Clear and compress: Computing persistent homology in chunks. In *Topological Methods in Data Analysis and Visualization III, Theory, Algorithms, and Applications*, pages 103–117. Springer, 2014.
- [5] Ulrich Bauer, Michael Kerber, Jan Reininghaus, and Hubert Wagner. Phat - persistent homology algorithms toolbox. *Journal of Symbolic Computation*, 78:76–90, 2017.
- [6] Paul Bendich, J.S. Marron, Ezra Miller, Alex Pieloch, and Sean Skwerer. Persistent homology analysis of brain artery trees. *Annals of Applied Statistics*, 10:198–218, 2016.
- [7] Silvia Biasotti, Andrea Cerri, Patrizio Frosini, and Daniela Giorgi. A new algorithm for computing the 2-dimensional matching distance between size functions. *Pattern Recognition Letters*, 32(14):1735–1746, 2011.
- [8] Mickaël Buchet, Frédéric Chazal, Tamal K. Dey, Fengtao Fan, Steve Y. Oudot, and Yusu Wang. Topological analysis of scalar fields with outliers. In *31st International Symposium on Computational Geometry (SoCG 2015)*, pages 827–841, 2015.
- [9] Chen Cai, Woojin Kim, Facundo Mémoli, and Yusu Wang. Elder-rule-staircodes for augmented metric spaces. In *36th International Symposium on Computational Geometry (SoCG 2020)*, pages 26:1–26:17, 2020.
- [10] Gunnar Carlsson and Afra Zomorodian. The theory of multidimensional persistence. *Discrete & Computational Geometry*, 42(1):71–93, 2009.
- [11] Chao Chen and Michael Kerber. Persistent homology computation with a twist. In *European Workshop on Computational Geometry (EuroCG)*, pages 197–200, 2011.
- [12] Aruni Choudhary, Michael Kerber, and Sharath Raghvendra. Improved topological approximations by digitization. In *Proceedings of the Thirtieth Annual ACM-SIAM Symposium on Discrete Algorithms, SODA*, pages 2675–2688, 2019.
- [13] Alex Cole and Gary Shiu. Topological data analysis for the string landscape. *Journal of High Energy Physics*, 2019(54), 2019.
- [14] René Corbet, Ulderico Fugacci, Michael Kerber, Claudia Landi, and Bei Wang. A kernel for multi-parameter persistent homology. *Computers & Graphics: X*, 2, 2019.
- [15] René Corbet and Michael Kerber. The representation

- theorem of persistence revisited and generalized. *Journal of Applied and Computational Topology*, 2:1–31, 2018.
- [16] Vin de Silva, Dmitriy Morozov, and Mikael Vejdemo-Johansson. Dualities in persistent (co)homology. *Inverse Problems*, 27(12):124003+, 2011.
- [17] Tamal Dey, Fengtao Fan, and Yusu Wang. Computing topological persistence for simplicial maps. In *30th International Symposium on Computational Geometry (SoCG 2014)*, pages 345–354, 2014.
- [18] Tamal Dey and Cheng Xin. Generalized persistence algorithm for decomposing multi-parameter persistence modules. arXiv:1904.03766, 2019.
- [19] Herbert Edelsbrunner and Georg Osang. The multi-cover persistence of Euclidean balls. In *34th International Symposium on Computational Geometry (SoCG 2018)*, pages 34:1–34:14, 2018.
- [20] David Eisenbud. *Commutative Algebra: With a View Toward Algebraic Geometry*. Graduate Texts in Mathematics. Springer, 1995.
- [21] Ulderico Fugacci and Michael Kerber. Chunk reduction for multi-parameter persistent homology. In *35th International Symposium on Computational Geometry (SoCG 2019)*, pages 23:1–23:13, 2019.
- [22] Clément Jamin, Sylvain Pion, and Monique Teillaud. 3D triangulations. In *CGAL User and Reference Manual*. CGAL Editorial Board, 5.0.3 edition, 2020.
- [23] Lida Kanari, Paweł Dłotko, Martina Scolamiero, Ran Levi, Julian Shillcock, Kathryn Hess, and Henry Markram. A topological representation of branching neuronal morphologies. *Neuroinformatics*, 16:3–13, 2018.
- [24] Michael Kerber, Michael Lesnick, and Steve Oudot. Exact computation of the matching distance on 2-parameter persistence modules. In *35th International Symposium on Computational Geometry (SoCG 2019)*, pages 46:1–46:15, 2019.
- [25] Michael Kerber, Dmitriy Morozov, and Arnur Nigmatov. Geometry helps to compare persistence diagrams. *ACM Journal of Experimental Algorithmics*, 22, 2017.
- [26] Michael Kerber and Arnur Nigmatov. Efficient approximation of the matching distance for 2-parameter persistence. In *36th International Symposium on Computational Geometry (SoCG 2020)*, pages 53:1–53:16, 2020.
- [27] Michael Lesnick. The theory of the interleaving distance on multidimensional persistence modules. *Foundations of Computational Mathematics*, 15(3):613–650, 2015.
- [28] Michael Lesnick and Matthew Wright. Computing minimal presentations and bigraded Betti numbers of 2-parameter persistent homology. arXiv:1902.05708, 2019.
- [29] Nina Otter, Mason A. Porter, Ulrike Tillmann, Peter Grindrod, and Heather A. Harrington. A roadmap for the computation of persistent homology. arXiv:1506.08903, 2015.
- [30] Florian T. Pokorny, Majd Hawasly, and Subramanian Ramamoorthy. Multiscale topological trajectory classification with persistent homology. In *Proceedings of Robotics: Science and Systems*, 2014.
- [31] Erik Rybakken, Nils Baas, and Benjamin Dunn. Decoding of neural data using cohomological feature extraction. *Neural Computation*, 31:68–93, 2019.
- [32] Sara Scaramuccia, Federico Iuricich, Leila De Floriani, and Claudia Landi. Computing multiparameter persistent homology through a discrete Morse-based approach. *Computational Geometry: Theory and Applications*, 89, 2020.
- [33] Donald R. Sheehy. Linear-size approximation to the Vietoris-Rips filtration. *Discrete & Computational Geometry*, 49:778–796, 2013.
- [34] Ann E. Sizemore, Jennifer E. Phillips-Cremens, Robert Ghrist, and Danielle S. Bassett. The importance of the whole: Topological data analysis for the network neuroscientist. *Network Neuroscience*, 3(3):656–673, 2019.
- [35] T. Sousbie, C. Pichon, and H. Kawahara. The persistent cosmic web and its filamentary structure. *Monthly Notices of the Royal Astronomical Society*, 414(1):384–403, 06 2011.
- [36] The RIVET Developers. Rivet. <http://rivet.online>, 2018.
- [37] Oliver Vipond. Multiparameter persistence landscapes. *Journal of Machine Learning Research*, 21(61):1–38, 2020.

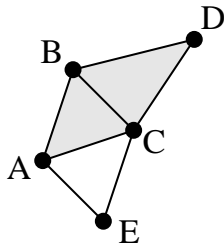


Figure 2: Example of a simplicial complex.

A Simplicial bifiltrations: a running example

For readers not familiar with some of the concepts underlying this work, we develop a running example on which we are illustrating most of the basic concepts needed in this work. We are rather verbose here, and readers familiar with basics of computational topology can probably read over the first subparagraph quite quickly.

Simplicial complexes and homology A *simplicial complex* C over a finite vertex set V is a collection of non-empty subsets of V that is closed under taking subsets. Elements of the complex of cardinality $k + 1$ are called k -*simplices*, and k is the dimension of the simplex. Simplices of dimension 0, 1, and 2, are called *vertices*, *edges*, and *triangles*, respectively. The dimension of a simplicial complex C is the maximal dimension of its faces. In Figure 2, we see a 2-dimensional simplicial complex over $V = \{A, B, C, D, E\}$, consisting of 5 vertices, 7 edges and 2 triangles. Clearly, this is generalizing the notion of a graph, as a graph is a simplicial complex of dimension 1. We call a k -simplex τ a *facet* of a $(k + 1)$ -simplex σ if $\tau \subset \sigma$.

Fixing a simplicial complex C and a dimension k , the $(k + 1, k)$ -*boundary matrix* is a matrix where every column corresponds to a $(k + 1)$ -simplex of C , every row corresponds to a k -simplex of C , and the (i, j) -entry is 1 if the k -simplex in row i is a facet of the $(k + 1)$ -simplex in column j . The simplicial complex depicted in Figure 2 is fully described by the pair (A, B) with A its $(2, 1)$ -boundary matrix and B its $(1, 0)$ -boundary matrix, given as

$$A = \begin{array}{c|cc} & ABC & BCD \\ \hline AB & 1 & 0 \\ AC & 1 & 0 \\ AE & 0 & 0 \\ BC & 1 & 1 \\ BD & 0 & 1 \\ CD & 0 & 1 \\ CE & 0 & 0 \end{array}$$

$$B = \begin{array}{c|ccccccc} & AB & AC & AE & BC & BD & CD & CE \\ \hline A & 1 & 1 & 1 & 0 & 0 & 0 & 0 \\ B & 1 & 0 & 0 & 1 & 1 & 0 & 0 \\ C & 0 & 1 & 0 & 1 & 0 & 1 & 1 \\ D & 0 & 0 & 0 & 0 & 1 & 1 & 0 \\ E & 0 & 0 & 1 & 0 & 0 & 0 & 1 \end{array}$$

Generally, a simplicial complex of dimension d is described by d such matrices.

Besides representing the complex, the matrices can be used to obtain further information using linear algebra. For instance, the union of the two triangles ABC , BCD can be written as the vector $v := (1, 1)^T$, and matrix-vector multiplication yields $Av = (1, 1, 0, 0, 1, 1, 0)$, corresponding to the edges AB , AC , BC , BD , which are precisely the four edges bounding the quadrilateral formed by the union of the two triangles. Similarly, the three edges AC , BC , BD form a path, and using the vector $w := (0, 1, 0, 1, 1, 0, 0)^T$, we get $Bw = (1, 0, 0, 1, 0)^T$, corresponding to the vertices A and D , which are the endpoints of the path. Note that in these examples, we exploit the fact that we interpret our matrices to be over $K = \mathbb{Z}_2$; a generalization is possible, but requires introducing orientations of simplices.

Using the three edges AB , AC , BC , we see that the corresponding vector z_1 satisfies $Bz_1 = 0$. This makes sense because the three edges form a cycle in the graph, hence there is no “boundary”. The same is true for the vector z_2 formed by BC , BD , CD , and this implies that the matrix product $B \cdot A$ is the zero matrix. This is not a coincidence, but the so-called *fundamental lemma of homology*, stating this to be true for every simplicial complex and two boundary matrices in consecutive dimensions. In other words, we have that the image of A is contained in the kernel of B . However, we can observe the kernel of B is larger, since it also contains, for instance, the vector z_3 formed by AC , AE , CE (we leave the translation to the actual vector in \mathbb{Z}_2^7 to the reader from now on). We can furthermore observe that $\{z_1, z_2, z_3\}$ is a basis of the kernel of B , which translates into the fact that every cycle in the graph can be obtained as a symmetric difference of the 3 corresponding cycles. We are interested in the difference of the kernel of B and the image of A , given by the quotient space

$$H_1 := \ker B / \text{im} A$$

which in this case is one-dimensional and can be represented by the cycle z_3 . This is called the *homology group* of the simplicial complex in dimension 1. As we deal with a base field (as opposed to integer coefficients as in the classical theory), the homology group is in fact a vector space, but we still use the standard notation. Intuitively, H_1 captures the cycles of the simplicial complex which are “non-trivial”, in the sense that they are

not bounded by a set of triangles. In our example, this is clearly the case for z_3 , but not for z_1 or z_2 .

Bi-filtrations and graded matrices We introduce more structure by giving every simplex a (bi-)grade in \mathbb{Z}^2 . This assigns a grade to each row and column of A and B , turning them into graded matrices. A possible assignment for our running example would be

		ABC	BCD					
		$(2, 2)$	$(3, 3)$					
$A =$	AB	$(1, 1)$	1	0				
	AC	$(2, 2)$	1	0				
	AE	$(2, 3)$	0	0				
	BC	$(1, 1)$	1	1				
	BD	$(1, 2)$	0	1				
	CD	$(2, 1)$	0	1				
	CE	$(3, 2)$	0	0				

		AB	AC	AE	BC	BD	CD	CE
		$(1, 1)$	$(2, 2)$	$(2, 3)$	$(1, 1)$	$(1, 2)$	$(2, 1)$	$(3, 2)$
$B =$	A	$(1, 1)$	1	1	0	0	0	0
	B	$(1, 1)$	1	0	0	1	0	0
	C	$(1, 1)$	0	1	0	1	0	1
	D	$(1, 1)$	0	0	0	0	1	0
	E	$(2, 2)$	0	0	1	0	0	1

Perhaps more illustrative, the same data can be displayed by a two-dimensional sequence of simplicial complexes as depicted in Figure 3. In here, at each grade (x, y) , we draw all simplices whose grade is $\leq (x, y)$ in the defined partial order over \mathbb{R}^2 . The simplices whose grade is equal to (x, y) are drawn in red. Recall that we required that for a column with grade g , with an 1-entry in a row with grade g' , $g' \leq g$ must hold. This translates into the property that at every grade g , the collection of simplices collected in this way forms a simplicial complex. This data is called a *bifiltration* of a simplicial complex and can be used to model the evolution of data when two scale parameters are varied independently from each other.

We can redo the same computation as before for any fixed grade now: for instance, on grade $p := (2, 2)$, we obtain $A_{\leq p}$, which is A from above with column 2 and rows 3 and 7 removed. $B_{\leq p}$ is B with columns 3 and 7, and row 5 removed. The kernel of $B_{\leq p}$ is spanned by z_1 and z_2 , the image of $A_{\leq p}$ by z_1 , and hence, the quotient group is one-dimensional, represented by z_2 . We can do similar calculations for each grade and obtain the homology group for each grade, which is depicted in the lower-right corners in Figure 3. Revisiting the definition of the persistence module represented by the two graded matrices (A, B) , these homology groups are precisely the vector spaces V_p in the definition of Section 2.

We stress out the the persistence module contains more information than just the homology on each grade. In some sense, the information is encoded more in the maps between the grades than in the grades themselves. As an example, set $p := (2, 2)$ and $p' := (3, 3)$. Recall

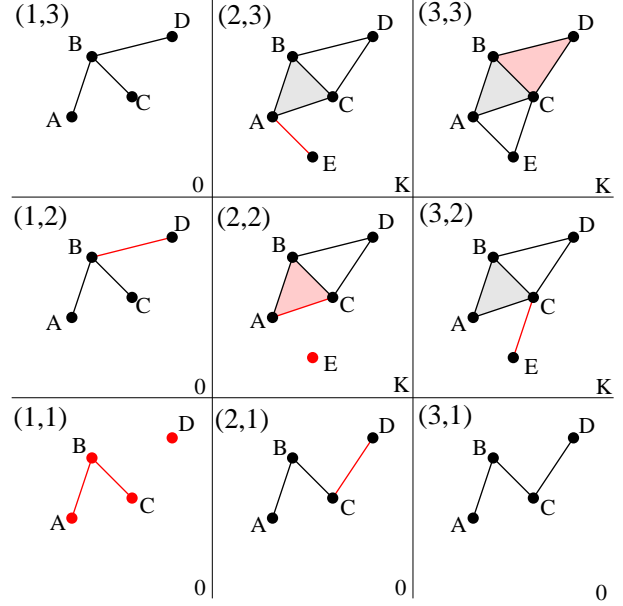


Figure 3: Example of a bifiltration. The upper left corner denotes the grade, the lower-right denotes the homology group of the complex.

that $\ker B_{\leq p}$ is generated by z_2 . The map $f_{p \rightarrow p'}$ is defined just by mapping z_2 to z_2 in $\ker B_{\leq p'}$, which represents a trivial element in the homology group because z_2 is bounded by a triangle at grade $(3, 3)$. That means that the generator at grade $(2, 2)$ becomes trivial at grade $(3, 3)$, meaning that although the vector spaces are isomorphic at both grades, the generators is changing. In contract, considering $p'' = (3, 2)$, the map $f_{p \rightarrow p''}$ maps generator to generator, because z_2 generates the homology group at scale $(3, 2)$.

We also point out that there is nothing special about the case of triangle, edges, and vertices: the entire approach generalizes to higher dimensions considering any two consecutive boundary matrices of a simplicial complex.

Conversion to a minimal presentation. We exemplify the conversion of (A, B) as given above into a minimal presentation, which is the goal of our algorithm. The main point is to identify a graded basis Z of $\ker B$, that is, a basis with a bi-grade for each element, such that $Z_{\leq p}$, denoting the basis elements of Z with grade $\leq p$, is a basis of $\ker B_{\leq p}$ for all p . Such a basis always exists, but this is non-trivial to prove (it follows from the fact that the kernel of a map between free $K[x, y]$ -modules is free, where $K[x, y]$ is the polynomial ring with two variables). In our example, however, such a graded kernel can be read off immediately: We pick $\{z_1, z_2, z_3\}$, where as above, z_1 is the cycle AB ,

AC , BC , z_2 is the cycle BC BD , CD and z_3 is the cycle AC , AE , CE , and we assign the grades $(2, 2)$ to z_1 and to z_2 , and $(3, 3)$ to z_3 . The procedure `Ker_basis` of Section 3 yields such a graded basis in general.

Since $B_{\leq p}A_{\leq p} = 0$, every column of A at grade p can be expressed as a linear combination of the basis elements from above of grades $\leq p$. In our case, this is very simple: The boundary of the triangle ABC is equal to z_1 , and the boundary of the triangle BCD is equal to z_2 . Written as graded matrix, this yields

$$M' = \begin{array}{c|cc} & ABC & BCD \\ & (2, 2) & (3, 3) \\ \hline z_1 & (2, 2) & 1 & 0 \\ z_2 & (2, 2) & 0 & 1 \\ z_3 & (3, 3) & 0 & 0 \end{array}$$

In general, this step requires to solve a linear system for every column, and the procedure `Reparam` of Section 3 is solving these systems in general.

The matrix M' is a presentation of the same persistence module as given by (A, B) . For example, at grade $p = (2, 2)$, we restrict ourselves to rows and columns of grade $\leq p$, which are column 1 and row 1 and 2. Hence, using the definition from Section 2, we get

$$V_p = \langle z_1, z_2 \rangle / \langle z_1 \rangle$$

which means that V_p is spanned by z_2 . Similarly, for $q = (3, 3)$, we obtain V_q to be spanned by z_3 , and it can be readily checked that the vector spaces, and maps in-between coincide at each grade with the ones defined by the matrix pair (A, B) .

While it does not happen in our small example, it may happen that columns of B give rise to superfluous relations (=columns) in the presentation matrix. This is the case whenever a column of grade p can be expressed as linear combination of other columns of grade $\leq p$. The smallest such example would be an example including the 4 boundary triangles of a tetrahedron on the same grade, where the last triangle added is just the sum of the other three. The procedure `Min_gens` filters out these superfluous relations in the general case.

The matrix M' is much succinct description of the persistence module compared to (A, B) , but it is still not minimal. The reason is that the kernel element z_1 is created at scale $(2, 2)$, but the the triangle ABC is also created at $(2, 2)$, including the element into the image of A (and hence trivializing it) right away. In the example, we can just remove the first row and column and arrive at

$$M = \begin{array}{c|c} & BCD \\ & (3, 3) \\ \hline z_2 & (2, 2) & 1 \\ z_3 & (3, 3) & 0 \end{array}$$

which is a minimal presentation. Indeed, re-considering Figure 3, we can summarize the situation as: there is a non-trivial cycle coming into existence at grade $(2, 2)$ which gets filled up at grade $(3, 3)$, and there is another non-trivial cycle starting at grade $(3, 3)$, which is never filled up.

In general, we cannot just remove a row and column from a presentation: we first have to ensure that every other column is re-expressed that the row to be removed does not appear as row index. Mathematically, that means to change the basis of $\text{in}B$; the procedure `minimize` performs this removal in general.

B Correctness

Correctness of lazy minimization. We first reformulate the definition of a minimal presentation of a persistence module in terms of commutative algebra. For more details on this perspective, see [28]. In this language, a *persistence module* is a \mathbb{Z}^2 -graded $K[x, y]$ -module, where $K = \mathbb{Z}_2$ as before, and a *presentation* of a persistence module M is a homomorphism $p : F^1 \rightarrow F^0$ between free persistence modules such that $\text{coker}(p) \cong M$. We say that a *basis* for a free persistence module is a minimal homogeneous set of generators. Let p be a presentation of M , and write $q : F^0 \rightarrow M$ for the canonical map; the presentation is *minimal* if (1) q maps a basis of F^0 bijectively to a minimal homogenous set of generators of M , and (2) p maps a basis of F^1 bijectively to a minimal homogenous set of generators of $\ker(q)$. This definition agrees with the definition of [28] by the analogue for persistence modules of [20, Lemma 19.4]. Any presentation of a persistence module M can be obtained (up to isomorphism) from a minimal presentation p by taking the direct sum with maps of the form $\text{id}_H : H \rightarrow H$ or of the form $H \rightarrow 0$, where H is free. Following Lesnick-Wright, we say that a presentation is *semi-minimal* if it can be obtained from a minimal presentation by taking the direct sum with maps of the form $\text{id}_H : H \rightarrow H$, where H is free.

If $p : F^1 \rightarrow F^0$ is a presentation of M , and we choose ordered bases B^0 and B^1 of F^0 and F^1 , then we can represent p by a bi-graded matrix P , and we abuse notation by also calling this bi-graded matrix a presentation of M . We write $P(i, j)$ for the entry of P in position (i, j) , and we write $P(*, j)$ for the j^{th} column of P .

PROPOSITION B.1. *If P is a semi-minimal presentation of a persistence module M , and P' is the bi-graded matrix obtained from P by the lazy minimization algorithm, then P' is a minimal presentation of M .*

Proof. We first show that P' is still a presentation of M . For this, we observe first that if k and j are

column indices of P , with $k \neq j$ and such that the grade of column k is less than or equal to the grade of column j (in the usual partial order on \mathbb{Z}^2), then adding column k of P to column j corresponds to multiplying P on the right with a bi-graded elementary matrix, and therefore does not change the isomorphism type of the cokernel. It follows that the column operations performed by the lazy minimization algorithm do not change the isomorphism type of the cokernel.

Now, if P has a row q and a column j that both have grade $\mathbf{z} = (z_1, z_2)$, such that $P(q, j) = 1$, and every other entry in row q and column j is zero, then we can remove row q and column j from P without changing the isomorphism type of the cokernel; this corresponds to removing a direct summand of the form $\text{id}_H : H \rightarrow H$, where H is a free persistence module on one generator at grade \mathbf{z} . Furthermore, the assumption that column j has only one non-zero entry can be weakened. Assume now that P has a column j with pivot q , both with grade \mathbf{z} , and such that $P(q, k) = 0$ for all $k \neq j$. Let $C = (q_1, \dots, q_r, q)$ be the row indices in which column j is non-zero, and say that P represents a homomorphism $p : F^1 \rightarrow F^0$, with respect to ordered bases $B^0 = (B_1^0, \dots, B_m^0)$ and $B^1 = (B_1^1, \dots, B_n^1)$. Define a basis $\tilde{B}^0 = (\tilde{B}_1^0, \dots, \tilde{B}_m^0)$ of F^0 , where $\tilde{B}_t^0 = B_t^0$ for $t \neq q$, and

$$\tilde{B}_q^0 = \sum_{s \in C} x^{z_1 - \text{gr}(s)_1} y^{z_2 - \text{gr}(s)_2} B_s^0.$$

If \tilde{P} represents p with respect to the bases \tilde{B}^0 and B^1 , then $\tilde{P}(*, k) = P(*, k)$ for all $k \neq j$, and $\tilde{P}(*, j)$ has a 1 in row q and zero elsewhere. So, by first replacing B^0 with \tilde{B}^0 , we can remove row q and column j from P without changing the isomorphism type of the cokernel. In the last step of the lazy minimization algorithm, in which all marked row-column pairs are removed, if we remove these row-column pairs in order of decreasing row index, then the previous argument shows that each row-column removal does not change the isomorphism type of the cokernel. This completes the proof that P' is still a presentation of M .

Finally, we show that P' is minimal. Since the LW minimization algorithm produces a minimal presentation from P , it suffices to show that the lazy minimization algorithm removes the same number of row-column pairs at each grade as the LW minimization algorithm. So, let \mathbf{z} be a grade of a column of P , and let $P_{\mathbf{z}}$ be the sub-matrix of P consisting of the columns and rows of P with grade \mathbf{z} . To complete the proof, we show that the number of row-column pairs with grade \mathbf{z} removed by the LW minimization algorithm and the number of row-column pairs with grade \mathbf{z} removed by the lazy minimization algorithm are both equal to the rank of the matrix $P_{\mathbf{z}}$. Say that a matrix N has the “distinct pivot”

property if any pair of non-zero columns of N have distinct pivots. Note that if N has the distinct pivot property, then the rank of N is the number of non-zero columns of N . The column operations performed by the LW minimization algorithm do not change the rank of $P_{\mathbf{z}}$, and after performing all column operations, the sub-matrix $P_{\mathbf{z}}$ has the distinct pivot property, and the columns with grade \mathbf{z} removed by the LW minimization algorithm are the non-zero columns of this matrix. Similarly, the column operations performed by the lazy minimization algorithm do not change the rank of $P_{\mathbf{z}}$, and after performing all column operations, the sub-matrix $P_{\mathbf{z}}$ has the distinct pivot property, and the columns with grade \mathbf{z} removed by the lazy minimization algorithm are the non-zero columns of this matrix. \square

Correctness of queuing. The correctness of the two techniques using priority queues follows more or less directly from the description given in the main body. We still give a formal proof for completeness. We start with the priority queue for the grades, assuming that each grade is handled by scanning all columns from left to right as in the RIVET algorithm.

PROPOSITION B.2. *Using a priority queue for the grades as described, the algorithms `min_gens` and `ker_basis` produce the same output as in the LW algorithm.*

Proof. The argument is mostly the same for `min_gens` and `ker_basis`, and we just talk about “the algorithm” for either of them. More precisely, we refer to the LW version of the algorithm and the optimized version of the algorithm when talking about the variant without and with the priority queue, respectively.

We call a grade (x, y) *significant* if the algorithm, on grade (x, y) performs a column operation on the matrix or appends a column to the output matrix. We show that every significant grade in the LW algorithm is added to the priority queue in the optimized version. That proves that the outcome is the same using an inductive argument.

Fix a grade (x, y) and assume that the algorithm (in the LW version) performs a column operation in this iteration. Let i be the smallest index on which such an operation is performed, let j be its pivot, and let (x', y) be its grade with $x' \leq x$. If $x' = x$, then there is a matrix column with grade (x, y) and the grade is pushed into the grade priority queue initially. Otherwise, if $x' < x$, column i has been reduced previously in grade $(x-1, y)$, and the reduction ended with $\rho(j) = i$ (otherwise, a further column addition would have been performed). The fact that a column addition is needed at grade (i, j) means that $\rho(j)$ must have been re-set, to an index

smaller than i . However, between $(x-1, y)$ and (x, y) , the algorithms iterated over the grades $(x-1, y+1), (x-1, y+2), \dots, (x-1, Y), (x, 1), (x, 2), \dots, (x, y-1)$ with Y the maximal y -grade. Note that in the first part of the sequence, with x -grade $x-1$, only columns with index $> i$ are updated because the matrix is stored in colex order. Hence, none of these iterations can set $\rho(j)$ to a smaller index. It follows that the update of $\rho(j)$ happens at a grade with x -grade x . But then, the updated reduction algorithm ensures when $\rho(j)$ is updated, the grade (x, y) is added to the priority queue in this step.

It remains the case that at grade (x, y) , the algorithm appends an output element. If the algorithm is `min_gens`, this only happens when the grade appears as matrix column, and as argued earlier, these grades are added to the priority queue. For `ker_basis`, an output column is added if a column is reduced from non-zero to zero, and this implies that at least one column addition was performed, so the grade is considered by the first part. \square

For the second queuing optimization (to avoid the left-to-right scan at each grade), the proof strategy is very similar:

PROPOSITION B.3. *Using one priority queue per y -grades as described, the algorithms `min_gens` and `ker_basis` produce the same output as in the LW algorithm.*

Proof. Again, we argue inductively that the same column operations are performed in the variant without and with priority queues. Fix a column i for which the LW variant (without priority queues) performs a column operation for grade (x, y) . It suffices to show that i is pushed to the priority queue for y . If i is at grade (x, y) , it is pushed by the algorithm as specified, so we can assume that its grade is (x', y) with $x' < x$.

Let j be the pivot of column i . As in the previous proof, the fact that a column addition is performed means that $\rho(j)$ has been updated during the algorithm since i was visited at grade $(x-1, y)$, and this can only happen at a grade (x, y') with $y' \leq y$. By the modified reduction method, i will be pushed into the priority queue of y in this case. \square

C Additional experimental data

In this section, we present further details on the experiments discussed in Section 5.

Function-Rips data. Along with the function-Rips bifiltration on a noisy circle point cloud, which was discussed in Section 5, we also considered the function-Rips bifiltration on a noisy 2-sphere in \mathbb{R}^3 ,

and created a persistence module by taking homology in dimension 2. The results are in Table 6. As was the case with the noisy circle, the runtime of the LW algorithm is dominated by `Min_gens`. And again, since some of these reductions can be performed during chunk preprocessing, which can be done in parallel, we obtain a running time improvement of a factor of around 8 in the largest example.

Mesh data from AIM@SHAPE. In Table 7 we display information about the size of the datasets we consider. The numbers ℓ, n, m give the size of the input, as in Section 2, and X, Y are the number of grades, as in Section 3. Time and memory consumption are displayed in Table 8. The rivet clone runs out of memory for all but the smallest instance, due to the large grid that needs to be created without the sparse grid optimization. Similar to the examples in Section 4, we see a clear advantage of using chunk preprocessing, both with respect to time and memory. On the other hand, neither parallelization nor the clearing optimization (not shown in the table) seem to improve the algorithm's performance for these instances.

Random Delaunay triangulations, $d = 2$. It might be surprising at first that the resulting presentation for this case is empty for all instances (Tables 9 and 10). To explain this, note that every generator in such a presentation corresponds to a void in the data at some grade $p = (x, y)$ which is bounded by a set of triangles of grade $\leq p$. Set $P := (-\infty, x) \times (-\infty, y) \times \mathbb{R}$. In other words, the void is a polyhedron whose vertices lie in P . Since P is a convex set, this implies that the void is contained in P as well. On the other hand, the void is triangulated by tetrahedra which are not present at grade p , as otherwise there would not be a void. But this is a contradiction, since for any such tetrahedron, its vertices are all in P , and hence so is the tetrahedron, by the way the grades are assigned. It follows that such a void does not exist.

N	Variant	IO	Ch	MG	KB	RP	Min	Time	Mem	Size
271K	rivet_clone	0.29	-	11.1	0.08	0.03	1.60	13.1	336MB	(7.8, 4.2)
	+queue,lazy	0.31	-	10.1	0.06	0.03	0.00	10.5	336MB	
	+chunk	0.30	9.85	0.12	0.00	0.00	0.00	10.3	406MB	
	+parfor	0.31	2.32	0.11	0.00	0.00	0.00	2.78	424MB	
522K	rivet_clone	0.56	-	41.0	0.20	0.06	5.72	47.6	861MB	(8.6, 5.6)
	+queue,lazy	0.56	-	37.0	0.15	0.06	0.01	37.8	863MB	
	+chunk	0.57	35.7	0.47	0.02	0.00	0.00	36.8	1.05GB	
	+parfor	0.60	7.32	0.35	0.00	0.00	0.00	8.31	1.11GB	
1.03M	rivet_clone	1.10	-	136	0.50	0.12	19.2	157	2.20GB	(11.0, 6.8)
	+queue,lazy	1.11	-	122	0.38	0.12	0.02	123	2.20GB	
	+chunk	1.11	117	1.66	0.10	0.00	0.00	120	2.70GB	
	+parfor	1.14	21.9	1.05	0.00	0.00	0.00	24.2	2.91GB	
2.12M	rivet_clone	2.30	-	573	1.46	0.30	70.9	648	6.39GB	(13.2, 9.0)
	+queue,lazy	2.32	-	508	1.18	0.30	0.08	512	6.40GB	
	+chunk	2.32	489	5.78	0.55	0.00	0.00	498	7.63GB	
	+parfor	2.38	84.7	2.74	0.00	0.00	0.00	90.0	8.15GB	
4.25M	rivet_clone	4.66	-	2090	4.41	0.75	299	2400	17.2GB	(21.0, 13.0)
	+queue,lazy	4.67	-	1839	3.74	0.75	0.28	1849	17.2GB	
	+chunk	4.71	1761	23.0	0.68	0.00	0.00	1790	20.7GB	
	+parfor	4.85	294	10.5	0.01	0.02	0.00	310	22.4GB	

Table 6: Time and memory consumption for the function-Rips bifiltration on a noisy 2-sphere. $N := \ell + n$ is the total number of columns in A and B . The meaning of the other columns is the same as in Table 4.

name	ℓ, n, m	X, Y	Size
hand	69K, 103K, 34K	33K, 34K	595×596
eros	953K, 1.4M, 477K	55K, 58K	$3K \times 3K$
dragon	1.3M, 2.0M, 656K	139K, 189K	$8K \times 8K$
raptor	2.0M, 3.0M, 1.0M	565K, 523K	$7K \times 7K$

Table 7: The statistics of the triangular mesh benchmark data. The numbers ℓ, n, m give the size of the input, X, Y are the number of grades, and “Size” is the size of the output.

name	Variant	IO	Ch	MG	KB	RP	Min	Time	Mem
hand	rivet_clone	0.37	-	34.2	37.8	0.07	12.0	84.8	8.79GB
	+queue,lazy	0.37	-	0.08	0.32	0.07	0.03	0.91	147MB
	+chunk	0.37	0.02	0.00	0.04	0.00	0.00	0.46	76MB
	+parfor	0.44	0.03	0.00	0.04	0.00	0.00	0.63	76MB
eros	queue,lazy	3.15	-	1.64	11.8	1.41	0.81	19.0	2.94GB
	+chunk	3.20	0.47	0.16	1.37	0.11	0.02	5.4	873MB
	+parfor	3.50	0.43	0.16	1.36	0.05	0.02	5.64	873MB
dragon	queue,lazy	5.58	-	2.84	14.0	2.03	1.18	26.0	3.40GB
	+chunk	5.34	0.78	0.34	2.21	0.20	0.06	9.05	1.17GB
	+parfor	5.70	0.70	0.32	2.23	0.11	0.05	9.23	1.17GB
raptor	queue,lazy	10.1	-	4.21	20.7	3.11	2.24	41.2	5.15GB
	+chunk	10.1	1.27	0.29	2.48	0.19	0.06	14.7	1.88GB
	+parfor	11.1	1.16	0.29	2.68	0.11	0.04	15.6	1.87GB

Table 8: Time and memory consumption for the triangular mesh dataset. The meaning of the columns is the same as in Table 4.

n	Variant	IO	Ch	MG	KB	RP	Min	Time	Mem	Size
5000	rivet_clone	0.14	-	1.28	0.99	0.02	2.69	5.16	242MB	(560.0, 282.4)
	+queue,lazy	0.14	-	0.09	0.06	0.03	0.01	0.35	55MB	
	+chunk	0.14	0.11	0.00	0.00	0.00	0.00	0.26	41MB	
	+parfor	0.15	0.05	0.00	0.00	0.00	0.00	0.21	39MB	
10000	rivet_clone	0.31	-	5.42	4.42	0.06	12.2	22.4	883MB	(1178.0, 593.2)
	+queue,lazy	0.30	-	0.22	0.15	0.06	0.04	0.80	120MB	
	+chunk	0.30	0.33	0.01	0.00	0.00	0.00	0.67	80MB	
	+parfor	0.30	0.14	0.01	0.01	0.00	0.00	0.47	79MB	
20000	rivet_clone	0.63	-	27.9	19.0	0.15	57.9	105	3.35GB	(2345.8, 1183.0)
	+queue,lazy	0.61	-	0.57	0.36	0.16	0.12	1.87	255MB	
	+chunk	0.62	1.04	0.04	0.02	0.00	0.00	1.75	158MB	
	+parfor	0.61	0.38	0.05	0.02	0.00	0.00	1.08	158MB	
40000	rivet_clone	1.54	-	150	93.7	0.36	415	661	13.0GB	(4703.0, 2374.0)
	+queue,lazy	1.28	-	1.54	0.85	0.36	0.37	4.46	577MB	
	+chunk	1.28	3.55	0.13	0.06	0.02	0.00	5.08	317MB	
	+parfor	1.25	1.12	0.13	0.06	0.00	0.00	2.61	317MB	

Table 9: Random Delaunay triangulations with $d = 1$, small instances. The meaning of the columns is the same as in Table 4.

n	Variant	IO	Ch	MG	KB	RP	Min	Time	Mem	Size
80000	queue,lazy	3.14	-	4.35	2.02	0.80	1.23	11.6	1.29GB	(9438.0, 4762.2)
	+chunk	2.70	13.2	0.40	0.17	0.08	0.01	16.6	715MB	
	+parfor	2.60	3.43	0.43	0.16	0.02	0.00	6.72	733MB	
160000	queue,lazy	6.58	-	12.2	4.69	1.95	4.77	30.4	2.80GB	(19275.8, 9722.6)
	+chunk	5.67	53.3	1.32	0.43	0.30	0.04	61.2	1.78GB	
	+parfor	5.47	11.3	1.46	0.41	0.07	0.02	18.9	2.04GB	
320000	queue,lazy	13.8	-	32.6	11.2	4.79	21.3	84.3	6.52GB	(38659.6, 19505.0)
	+chunk	11.8	227	4.69	1.20	1.28	0.12	247	4.80GB	
	+parfor	11.5	41.6	5.05	1.04	0.23	0.06	59.7	6.17GB	
640000	queue,lazy	29.4	-	85.0	26.0	11.2	94.6	247	14.7GB	(77704.2, 39200.4)
	+chunk	24.8	1019	18.1	3.95	6.11	0.44	1073	14.8GB	
	+parfor	24.0	169	18.8	2.93	0.99	0.22	217	20.1GB	

Table 10: Random Delaunay triangulations with $d = 1$, large instances. The meaning of the columns is the same as in Table 4.

n	Variant	IO	Ch	MG	KB	RP	Min	Time	Mem	Size
5000	rivet_clone	0.14	-	0.89	1.90	0.03	2.83	5.81	314MB	(0.0, 0.0)
	+queue,lazy	0.14	-	0.01	0.28	0.03	0.00	0.49	127MB	
	+chunk	0.14	0.01	0.00	0.05	0.00	0.00	0.21	42MB	
	+parfor	0.15	0.01	0.00	0.05	0.00	0.00	0.22	41MB	
10000	rivet_clone	0.30	-	3.88	8.42	0.06	12.2	24.9	1.07GB	(0.0, 0.0)
	+queue,lazy	0.30	-	0.04	0.79	0.07	0.02	1.25	306MB	
	+chunk	0.29	0.02	0.00	0.14	0.00	0.00	0.46	82MB	
	+parfor	0.29	0.03	0.00	0.14	0.00	0.00	0.48	85MB	
20000	rivet_clone	0.62	-	19.3	49.8	0.16	57.3	127	3.89GB	(0.0, 0.0)
	+queue,lazy	0.62	-	0.10	2.43	0.16	0.07	3.44	793MB	
	+chunk	0.62	0.07	0.00	0.37	0.00	0.00	1.08	184MB	
	+parfor	0.61	0.07	0.00	0.40	0.00	0.00	1.10	194MB	
40000	rivet_clone	1.54	-	109	260	0.40	391	764	14.5GB	(0.0, 0.0)
	+queue,lazy	1.24	-	0.24	7.64	0.41	0.18	9.81	2.13GB	
	+chunk	1.25	0.15	0.00	1.11	0.00	0.00	2.56	453MB	
	+parfor	1.24	0.14	0.00	1.17	0.00	0.00	2.61	475MB	

Table 11: Random Delaunay triangulations with $d = 2$, small instances. The meaning of the columns is the same as in Table 4.

n	Variant	IO	Ch	MG	KB	RP	Min	Time	Mem	Size
80000	queue,lazy	3.09	-	0.55	23.8	1.15	0.45	29.3	5.60GB	(0.0, 0.0)
	+chunk	2.63	0.33	0.01	3.34	0.02	0.00	6.40	1.12GB	
	+parfor	2.53	0.31	0.01	3.48	0.01	0.00	6.42	1.17GB	
160000	queue,lazy	6.40	-	1.24	79.2	3.52	1.45	92.4	14.8GB	(0.0, 0.0)
	+chunk	5.45	0.72	0.03	10.3	0.05	0.00	16.7	2.73GB	
	+parfor	5.26	0.67	0.03	10.5	0.03	0.00	16.6	2.83GB	
320000	queue,lazy	13.2	-	2.77	285	13.9	4.68	321	41.5GB	(0.0, 0.0)
	+chunk	11.3	1.57	0.08	35.9	0.13	0.01	49.4	7.41GB	
	+parfor	10.9	1.44	0.07	36.3	0.07	0.01	49.1	7.60GB	
640000	queue,lazy	28.0	-	6.28	1670	215	17.5	1941	64.9GB	(0.0, 0.0)
	+chunk	27.6	3.37	0.17	112	0.30	0.03	144	19.6GB	
	+parfor	22.5	3.03	0.15	113	0.16	0.02	140	19.9GB	

Table 12: Random Delaunay triangulations with $d = 2$, large instances. The meaning of the columns is the same as in Table 4.

N	Variant	IO	Ch	MG	KB	RP	Min	Time	Mem	Size
100K	rivet_clone	0.12	-	0.62	0.54	0.04	4.96	6.30	84MB	(6066.2, 3068.6)
	+queue,lazy	0.13	-	0.05	0.08	0.04	0.02	0.34	86MB	
	+chunk	0.12	0.02	0.01	0.01	0.01	0.00	0.21	39MB	
	+parfor	0.13	0.02	0.01	0.02	0.00	0.00	0.20	38MB	
199K	rivet_clone	0.25	-	2.61	2.27	0.11	21.7	27.0	207MB	(13029.8, 6588.8)
	+queue,lazy	0.26	-	0.10	0.21	0.11	0.06	0.77	210MB	
	+chunk	0.25	0.05	0.04	0.05	0.03	0.01	0.46	75MB	
	+parfor	0.25	0.04	0.04	0.05	0.01	0.01	0.44	87MB	
400K	rivet_clone	0.53	-	14.7	9.57	0.26	111	136	536MB	(27425.0, 13858.4)
	+queue,lazy	0.57	-	0.24	0.57	0.26	0.20	1.90	545MB	
	+chunk	0.53	0.13	0.09	0.14	0.08	0.05	1.06	174MB	
	+parfor	0.53	0.10	0.10	0.15	0.04	0.02	0.98	214MB	
801K	rivet_clone	1.13	-	91.8	50.9	0.65	697	842	1.31GB	(57810.4, 29202.0)
	+queue,lazy	1.20	-	0.54	1.46	0.65	0.57	4.52	1.32GB	
	+chunk	1.12	0.29	0.21	0.40	0.22	0.15	2.45	420MB	
	+parfor	1.11	0.21	0.22	0.42	0.12	0.08	2.19	528MB	

Table 13: Multi-cover data, small instances. $N := \ell + n$ is the total number of columns in A and B . The meaning of the other columns is the same as in Table 4.

N	Variant	IO	Ch	MG	KB	RP	Min	Time	Mem	Size
1.6M	queue,lazy	3.06	-	1.23	4.18	1.69	1.90	12.2	3.67GB	(119379.6, 60273.4)
	+chunk	2.38	0.60	0.49	1.21	0.61	0.50	5.86	1.15GB	
	+parfor	2.32	0.40	0.51	1.25	0.32	0.21	5.1	1.49GB	
3.17M	queue,lazy	7.26	-	2.81	11.6	4.61	6.20	32.9	9.50GB	(244096.4, 123224.4)
	+chunk	5.09	1.28	1.14	3.47	1.65	1.55	14.3	3.04GB	
	+parfor	4.98	0.86	1.19	3.50	0.74	0.54	11.9	4.07GB	
6.49M	queue,lazy	20.2	-	6.44	32.8	14.5	22.3	97.3	27.1GB	(509904.2, 257387.4)
	+chunk	11.4	2.80	2.69	10.1	4.72	5.10	37.2	8.78GB	
	+parfor	11.0	1.83	2.75	10.2	1.82	1.38	29.4	12.3GB	

Table 14: Multi-cover data, large instances. $N := \ell + n$ is the total number of columns in A and B . The meaning of the other columns is the same as in Table 4.

name, N	Variant	Vector	Heap	List	Set	A-Full	A-Set	A-Heap	A-Bit-Tree
multi-cover 1.59M	lazy, ..., chunk +parfor	6.56 5.42	24.5 18.5	17.8 16.2	23.7 19.2	12.0 9.04	21.0 15.8	22.3 15.8	7.43 5.81
multi-cover 6.49M	lazy, ..., chunk +parfor	37.8 28.6	189 138	166 118	180 141	82.0 60.9	185 135	169 118	45.9 35.6
func. Rips 1.02M	lazy, ..., chunk +parfor	6.73 4.64	22.5 11.4	29.4 21.5	16.9 9.71	11.0 5.88	16.1 7.86	24.0 10.5	8.33 4.03
func. Rips 8.17M	lazy, ..., chunk +parfor	108 65.7	435 211	698 539	288 162	180 89.0	277 131	459 198	125 50.6
hand 172K	lazy, ..., chunk +parfor	0.52 0.49	0.53 0.53	0.73 0.78	0.56 0.57	0.54 0.5	0.59 0.52	0.54 0.52	0.53 0.49
dragon 3.28M	lazy, ..., chunk +parfor	9.04 8.73	11.4 10.5	40.4 53.7	11.4 10.9	10.2 9.19	11.5 10.5	11.1 9.91	9.51 8.85
random Del. ($d = 1$) 1.68M	lazy, ..., chunk +parfor	16.9 6.73	50.8 14.0	104 29.5	34.5 12.3	22.6 8.25	32.5 11.6	51.0 13.1	17.1 6.37
random Del. ($d = 1$) 6.75M	lazy, ..., chunk +parfor	248 59.5	697 165	2381 630	451 138	295 79.6	431 150	687 152	213 53.8
random Del. ($d = 2$) 1.60M	lazy, ..., chunk +parfor	6.68 6.28	23.9 23.6	48.7 72.2	23.8 24.4	9.67 9.26	24.4 23.5	19.8 19.2	6.35 6.14
random Del. ($d = 2$) 6.43M	lazy, ..., chunk +parfor	52.1 49.9	254 251	1196 1620	262 266	70.1 68.1	312 274	196 193	38.9 38.0
convex hull 2.00M	lazy, ..., chunk +parfor	7.6 7.18	9.31 8.78	17.9 17.2	9.48 9.46	8.33 7.76	9.33 8.44	9.17 8.38	7.74 7.59
convex hull 8.00M	lazy, ..., chunk +parfor	32.3 29.6	42.3 39.0	158 119	42.5 40.8	36.2 33.8	45.3 38.9	41.4 39.0	32.5 30.7

Table 15: Running times for the different column types in PHAT. From left to right: $N := \ell + n$ is the total number of columns in A and B , `vector_vector`, `vector_heap`, `vector_list`, `vector_set`, `full_pivot_column`, `sparse_pivot_column`, `heap_pivot_column`, `bit_tree_pivot_column`.

D Clearing

The clearing optimization (also hinted at in [28]) is based on the following idea: When the algorithm `Min_gens` returns a column, by definition, the column encodes an element of the kernel of B . We would like to simply use this element as a basis vector instead of computing a different one through additional column operations in `Ker_basis`. Indeed, if the column has grade p , then it represents a kernel element at grade p . The problem, however, is that this kernel element might be present at grades smaller than p as well, and it seems difficult to determine the “birth grade” of this kernel element in general, and which kernel element in `ker_basis` can be replaced with that column.

There are cases, however, where this question can be resolved: call a non-zero column *pivot-dominated*, if each non-zero row entry of the column is at a grade that is smaller than the grade of the pivot. In particular, local columns are pivot-dominated. We then proceed as follows: At the beginning of `Ker_basis`, iterate over the columns returned by `Min_gens`. If a column is pivot-dominated with pivot i , we add this column to the kernel immediately, with the same grade as the row grade of i in A , and we set column i in B to zero (it is possible that the same column i is set by several columns of `Min_gens` – this does not invalidate the algorithm, since either of them yields a valid outcome).

LEMMA D.1. *The modified algorithm yields a valid kernel basis.*

Proof. Consider a pivot-dominated column c returned by `Min_gens`, with pivot index i at grade p . First, we argue that the unmodified `ker_basis` procedure will return a kernel element when visiting column i at grade p : indeed, this happens if and only if there is a linear combination in B that involves column i and other columns with grade $\leq p$. But since c is pivot-dominated, it encodes precisely such a linear combination. So, letting c' denote the column produced by the unmodified algorithm at column i , we have that c and c' differ by a linear combination of elements with index $< i$. Hence, exchanging c' with c yields a basis for the kernel of $B_{\leq p}$, and for all grades $\neq p$, the basis is unaffected. The statement follows by applying this argument iteratively. \square

The lemma implies that the resulting minimal presentation is still isomorphic to the original one, proving the correctness of the algorithm.

Practical evaluation. For most cases, the clearing optimization shows no practical benefit. There are several good reasons for this:

- The modification can only improve the performance of `ker_basis` (and potentially `reparam`) and hence is useless when `chunk` and/or `min_gens` are the computational bottleneck, as for instance the case in the function-Rips datasets (Table 5).
- When `Min_gens` returns much fewer columns than `ker_basis`, clearing will only save operations for a small fraction of columns. This happens in particular when A is much smaller than B .
- To take any effect, there must be many pivot-dominated columns. However, using `chunk` preprocessing, there will not be any local column returned by `Min_gens` which is the most common example of pivot-domination.

We observed that the fraction of pivot-dominated columns varies a lot between the examples. For instance, in our convex hull examples, as well as for the meshes, the number of such columns was very small (less than 5% of all columns from `Min_gens`). For random Delaunay complexes and homology dimension 2, there was not a single pivot-dominated columns throughout, whereas for dimension 1, more than 90% of the columns were pivot-dominated. Still, clearing has no significant effect in these examples either, because the majority of running time is spent on chunk preprocessing.

N	KB	KB*	Δ	MG
800K	0.42	0.34	0.08	0.24
1.6M	1.25	1.00	0.25	0.56
3.2M	3.50	2.76	0.74	1.29
6.5M	10.2	7.89	2.31	3.03

Table 16: The effect of the clearing optimization on the multi cover dataset. From left to right: $N := \ell + n$ is the total number of columns in A and B , time for `Ker_basis` without clearing, time for `Ker_basis` with clearing, absolute difference of running times, time for `Min_gens`.

The only type of example where we could observe an effect on practical performance was the multi-cover dataset: here, we observed that consistently about half of the columns returned by `Min_gens` are pivot-dominated. In Table 16, we see that clearing indeed yields speed-ups to `ker_basis`, due to a decrease in column additions.

Note that the clearing improvement requires that `Min_gens` terminates before `ker_basis` starts. Therefore, it cannot be combined with the previously mentioned option of running `Min_gens` and `ker_basis` in parallel. In this example, this parallel option leads to

slightly better results, as the last two columns in Table 16 show.

To summarize, many things have to come together to make clearing useful in practice; we do not rule out the possibility that instances exist where it leads to significant speedups, but such instances have to be identified in future work.

E Pseudocode

In this section, we give pseudocode for all the algorithms discussed in the paper. Algorithms 1–7 describe the LW algorithm, and Algorithms 8–13 our improved algorithm. More precisely, we describe the version here that uses chunk preprocessing, queues, and lazy minimization. We also marked the for loops in the pseudo-code that can be run in parallel.

Algorithm 1 Matrix reduction, LW-version

```
function REDUCE_LW( $A, i, use\_auxiliary = false$ )
  ▷  $A$  maintains a pivot vector  $piv$ 
  ▷  $piv[i] = k$  means that column  $k$  in  $A$  has pivot  $i$ .
  ▷  $piv[i] = -1$  means that no (visited) column in  $A$  has pivot  $i$ .
  ▷ If  $use\_auxiliary$  is set,  $A$  also maintains an auxiliary matrix.
  while column  $i$  in  $A$  is not empty do
     $j \leftarrow$  pivot of column  $i$ 
     $k \leftarrow piv[j]$ 
    if  $k = -1$  or  $k > j$  then
       $piv[j] \leftarrow i$ 
      break
    else
      add column  $k$  to column  $i$ 
      if  $use\_auxiliary$  then
        add auxiliary-column  $k$  to auxiliary-column  $i$ 
      end if
    end if
  end while
end function
```

Algorithm 2 Min_gens, LW-version

```
function MIN_GENS_LW( $A$ )
  ( $X, Y$ )  $\leftarrow$   $grid\_dim\_of(A)$ 
   $Out \leftarrow \emptyset$ 
  for  $x = 1, \dots, X$  do
    for  $y = 1, \dots, Y$  do
       $L \leftarrow$  column indices of  $A$  with grades  $(0, y), \dots, (x-1, y)$  in order
      for  $i \in L$  do
        REDUCE_LW( $A, i$ )
      end for
       $I \leftarrow$  column indices of  $A$  with grade  $(x, y)$ 
      for  $i \in I$  do
        REDUCE_LW( $A, i$ )
        if column  $i$  is not zero then
          Append column  $i$  to  $Out$  with grade  $(x, y)$ 
        end if
      end for
    end for
  end for
  return  $Out$ 
end function
```

Algorithm 3 Ker_basis, LW-version

```
function KER_BASIS_LW( $B$ )
  ( $X, Y$ )  $\leftarrow$  grid_dim_of( $B$ ) ▷ grades of  $B$  are on  $X \times Y$  grid
   $Out \leftarrow \emptyset$ 
  for  $x = 1, \dots, X$  do
    for  $y = 1, \dots, Y$  do
       $L \leftarrow$  column indices of  $A$  with grades  $(0, y), \dots, (x, y)$  in order
      for  $i \in L$  do
        REDUCE_LW( $A, i, use\_auxiliary = true$ )
        if column  $i$  has turned from non-zero to zero then
          Append auxiliary-column of  $i$  to  $Out$  with grade  $(x, y)$ 
        end if
      end for
    end for
  end for
  return  $Out$ 
end function
```

Algorithm 4 Reparameterize

```
function REPARAM( $G, K$ )
  ▷  $G$  is the output of MIN_GENs( $A$ )
  ▷  $K$  is the output of KER_BASIS( $B$ )
  Form matrix  $(K|G)$  by concatenation.
   $Out \leftarrow \emptyset$ 
  for  $i$  in index range of  $G$ -column in  $(K|G)$  do ▷ Parallelizable
    REDUCE_LW( $(K|G), i, use\_auxiliary = true$ ) ▷ Column  $i$  is zero afterwards
    Append the auxiliary column  $i$  to  $Out$ 
  end for
  return  $Out$ 
end function
```

Algorithm 5 Locality test

```
function IS_LOCAL( $A, i$ )
  if column  $i$  in  $A$  is 0 then
    return true
  end if
   $j \leftarrow$  pivot of column  $i$  in  $A$ 
  Return true iff the column grade of  $i$  in  $A$  equals the row grade of  $j$  in  $A$ 
end function
```

Algorithm 6 Minimization, LW-version

```
function MINIMIZE_LW( $M'$ )
   $n \leftarrow$  # columns in  $M'$ 
  for  $i = 1, \dots, n$  do
    if IS_LOCAL( $M', i$ ) then
       $j \leftarrow$  pivot of column  $i$  in  $M'$ 
      for  $k = i + 1, \dots, n$  do
        if column  $k$  in  $M'$  contains  $j$  as row index then
          Add column  $i$  to column  $k$ 
        end if
      end for
      Mark column  $i$  and row  $j$  in  $M'$ 
    end if
  end for
   $M \leftarrow$  submatrix of  $M'$  consisting of unmarked rows and columns
  Re-index the columns of  $M$  and return  $M$ 
end function
```

Algorithm 7 The LW-algorithm

```
function MIN_PRES_LW( $(A, B)$ )
   $G \leftarrow$  MIN_GENS_LW( $A$ )
   $K \leftarrow$  KER_BASIS_LW( $B$ )
   $M' \leftarrow$  REPARAM( $G, K$ )
   $M \leftarrow$  MINIMIZE_LW( $M'$ )
  return  $M$ 
end function
```

Algorithm 8 Matrix reduction, new version

function REDUCE_NEW($A, i, grade, use_auxiliary = false, local_check = false$)

▷ $grade$ is the grade that the algorithm is currently considering

▷ On top of pivot vector and auxiliary vector, A maintains priority queues:

▷ $cols_at_y_grade[y_0]$ is a priority queue for column indices at y -grade y_0

▷ $grade_queue$ is a priority queue of grades that the algorithm needs to look at

while column i in A is not empty **do**

$j \leftarrow$ pivot of column i

$k \leftarrow piv[j]$

if $k = -1$ **then**

$piv[j] \leftarrow i$

break

end if

if $k > j$ **then**

$y \leftarrow$ y -grade of column k in A

 Push k to $cols_at_y_grade[y]$

$x \leftarrow$ x -grade of $grade$

 Push (x, y) to $grade_queue$

$piv[j] \leftarrow i$

break

end if

if $local_check$ and not IS_LOCAL(A, i) **then**

break

end if

 add column k to column i

if $use_auxiliary$ **then**

 add auxiliary-column k to auxiliary-column i

end if

end while

end function

Algorithm 9 Min_gens, new version

```
function MIN_GENS_NEW( $A$ )
  Initialize  $grade\_queue$  as empty priority queue
  for each column  $c$  of  $A$  do
    Push the grade of  $c$  into  $grade\_queue$ 
  end for
  for each  $y$ -grade  $y_0$  that appears in a column of  $A$  do
    Initialize  $cols\_at\_y\_grade[y_0]$  as empty priority queue
  end for
   $Out \leftarrow \emptyset$ 
  while  $grade\_queue$  is not empty do
    Pop the grade  $(x, y)$  from  $grade\_queue$  minimal in lex order
    Push all column indices at grade  $(x, y)$  into  $cols\_at\_y\_grade[y]$ 
    while  $cols\_at\_y\_grade[y]$  is not empty do
      Pop column index  $i$  from  $cols\_at\_y\_grade[y]$  minimal in lex order
      REDUCE_NEW( $A, i, (x, y)$ ) ▷ Might change the priority queues as side effect
      if column  $i$  is not 0 and its grade is  $(x, y)$  then
        Append column  $i$  to  $Out$  with grade  $(x, y)$ 
      end if
    end while
  end while
  return  $Out$ 
end function
```

Algorithm 10 Ker_basis, new version

```
function KER_BASIS_NEW( $B$ )
  Initialize  $grade\_queue$  as empty priority queue
  for each column  $c$  of  $B$  do
    Push the grade of  $c$  into  $grade\_queue$ 
  end for
  for each  $y$ -grade  $y_0$  that appears in a column of  $B$  do
    Initialize  $cols\_at\_y\_grade[y_0]$  as empty priority queue
  end for
   $Out \leftarrow \emptyset$ 
  while  $grade\_queue$  is not empty do
    Pop the grade  $(x, y)$  from  $grade\_queue$  minimal in lex order
    Push all column indices at grade  $(x, y)$  into  $cols\_at\_y\_grade[y]$ 
    while  $cols\_at\_y\_grade[y]$  is not empty do
      Pop column index  $i$  from  $cols\_at\_y\_grade[y]$  minimal in lex order
      REDUCE_NEW( $A, i, (x, y), use\_auxiliary=true$ ) ▷ Might change the priority queues as side effect
      if column  $i$  has turned from non-zero to zero then
        Append auxiliary-column  $i$  of  $A$  to  $Out$  with grade  $(x, y)$ 
      end if
    end while
  end while
  return  $Out$ 
end function
```

Algorithm 11 Minimization, new version

function MINIMIZE_NEW(M') $n \leftarrow$ # columns in M' **for** $i = 1, \dots, n$ **do** $(x, y) \leftarrow$ grade of column i REDUCE_NEW($M', i, (x, y), \text{local_check}=\text{true}$)**if** IS_LOCAL(M', i) **then** $j \leftarrow$ pivot of column i Mark row j and column i **end if****end for****for** each unmarked column c **do** \triangleright Parallelizable $new_col \leftarrow$ empty list**while** c is not 0 **do**Get maximal index j from c **if** j is marked **then** $k \leftarrow piv[j]$ Add column k to c **else**Remove index j from c and append it to new_col **end if****end while**Set column i of M' to new_col **end for** $M \leftarrow$ submatrix of M' consisting of unmarked rows and columnsRe-index the columns of M and **return** M **end function**

Algorithm 12 Chunk preprocessing

```
function CHUNK( $(A, B)$ )
   $n \leftarrow$  # columns in  $A$ 
  for  $i = 1, \dots, n$  do
     $(x, y) \leftarrow$  grade of column  $i$  in  $A$ 
    REDUCE_NEW( $A, i, (x, y), \text{local\_check}=\text{true}$ )
    if IS_LOCAL( $A, i$ ) then
       $j \leftarrow$  pivot of column  $i$  in  $A$ 
      Mark row  $j$  and column  $i$  of  $A$  and mark column  $j$  of  $B$ 
    end if
  end for
  for each unmarked column  $c$  in  $A$  do ▷ Parallelizable
     $\text{new\_col} \leftarrow$  empty list
    while  $c$  is not 0 do
      Get maximal index  $j$  from  $c$  and remove it from  $c$ 
      if  $j$  is marked then
         $k \leftarrow \text{piv}[j]$ 
        Add column  $k$  to  $c$ 
      else
        Append index  $j$  to  $\text{new\_col}$ 
      end if
    end while
    Set column  $i$  of  $A$  to  $\text{new\_col}$ 
  end for
   $(A', B') \leftarrow$  submatrices of  $(A, B)$  consisting of unmarked rows and columns
  Re-index the columns of  $A'$  and  $B'$  and return  $(A', B')$ 
end function
```

Algorithm 13 The fast minimal presentation algorithm

```
function MIN_PRES_NEW( $(A, B)$ )
   $(A', B') \leftarrow$  CHUNK( $A, B$ )
   $G \leftarrow$  MIN_GENS_NEW( $A'$ )
   $K \leftarrow$  KER_BASIS_NEW( $B'$ )
   $M' \leftarrow$  REPARAM( $G, K$ )
   $M \leftarrow$  MINIMIZE_NEW( $M'$ )
  return  $M$ 
end function
```
